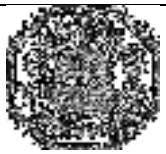

JAMILA


Joint mAster of Mediterranean Initiatives on renewabLe and sustainAble energy

Palestine Polytechnic University

Deanship of Graduate Studies and Scientific Research

Master Program of Renewable Energy and Sustainability

Enhancing Thermal Conductivity of Phase Change Materials Using Nanomaterials and its Effectiveness in Cooling Solar Cells.

By
Huda Albisher

Supervisor
Dr. Mustafa Abu-Safa

Thesis submitted in partial fulfillment of requirements of the degree

Master of Science in Renewable Energy & Sustainability

July, 2023

JAMILA

Joint mAster of Mediterranean Initiatives on renewable and sustainable energy

The undersigned hereby certify that they have read, examined and recommended to the Deanship of Graduate Studies and Scientific Research at Palestine Polytechnic University and the Faculty of Science at Al-Qdus University the approval of a thesis entitled:

Enhancing Thermal Conductivity of Phase Change Materials Using Nanomaterials and its Effectiveness in Cooling Solar Cells.

Submitted by

Huda Albisher

in partial fulfillment of the requirements for the degree of Master in Renewable Energy & Sustainability .

Graduate Advisory Committee:

Dr. Mustafa Abu-safa
(Supervisor), University (typed)
Signature: _____ Date: 31/8/2023

Dr. Maher Maghalseh
(Internal committee member), University (typed).
Signature: _____ Date: 5/9/2023

Dr. Jamal Ghabboun
(External committee member), University (typed).
Signature: _____ Date: 31/8/2023

Thesis Approved by:

Name: Dr. Nafez Naser Aldeen

Dean of Graduate Studies & Scientific Research

Palestine Polytechnic University

Signature:.....

Date:.....

ABSTRACT

With the recent increasing reliance on renewable energy, the interest in studying energy storage technologies is increased, because renewable energy is volatile and not available all the time. The latent heat storage system is considered the most promising technology in thermal energy storage because of its many advantages. The most important feature of these systems that they have the ability to store large amounts of thermal energy without a significant change in their temperature. This technique uses phase change material (PCM) as thermal energy storage medium. However, low thermal conductivity of PCM is the major drawback of the system. Previous studies indicated that adding nanomaterial additives to PCM for enhancing the thermal conductivity is one of the most common solutions for this problem.

Previous researches studied the possibility of using different types of materials as PCM, as well as the effect of different types of nano additives on their thermophysical properties. They focused on studying each nano-additive separately. Recently, limited number of studies have been published on the effect of using more than one type of nano-additives together (nanohybrid) on the thermophysical properties of PCM. Studies have shown that the addition of nanomaterials generally increases thermal conductivity of PCM.

On the other hand, researches tended to study the possibility of using enhanced PCM to cool solar cells. In fact, raising the solar cell operating temperature negatively impacts its efficiency. This problem is considered one of the biggest problems of solar energy systems that researches are still working to solve it. The researches' results about the ability to use paraffin as a PCM to cool solar cells were positive.

This thesis presents a study about using nano additives to improve the thermal conductivity of phase change materials and their ability to regulate the temperature of photovoltaic cell (PV) in a normal operating temperature range thus improve its efficiency.

This study is a continuation of previous researches. The effect of nanomaterials' shape that was added to PCM was taken into account. Therefore, this study focused on the possibility of enhancing the thermal conductivity of paraffin by adding different shapes of silver nanomaterials to it (silver nanoparticles, silver nanowires and nanohybrid with silver nanoparticles and silver nanowires). Nanomaterials were added at volume fractions 0.5% and 1%. Then, the study examined the ability to use this improved material on regulating and reducing the temperature of solar cells. We used the "Solidworks" program to create a 3D system, and then we used the "Ansys Fluent" software to simulate five cases:

- PV without PCM.
- PV with PCM.
- PV with PCM enhanced by nanoparticles.
- PV with PCM enhanced by nanowires.
- PV with PCM enhanced by nanohybrid (a mixture of nanoparticles and nanowires).

The thermophysical properties of PCM (which is temperature-dependent) were defined using a user-defined function (UDF). After that, they were compiled to the Ansys fluent solver. Then, we ran the simulation under a set of hypotheses that were taken into account.

The results of the five cases were analyzed and their ability to reduce PV temperature, and thus the raise in its efficiency were clarified. We found that the addition of nanowires at a volume fraction 1% led to the greatest improvement in the thermal conductivity of paraffin, but using PCM enhanced by nanowire at volume fraction 0.5% gave the best results in decreasing the temperature of PV. The average temperature of PV declined by 14.9 degrees (kelvin). In addition, the efficiency of PV rose about 7.6%. Followed by using PCM enhanced by nanoparticles at volume fraction 1%. The average temperature of PV declined by 12.9 degrees. Moreover, the efficiency of PV rose about 6.6%.

تحسين التوصيل الحراري للمواد متحولة الحالة الفيزيائية باستخدام الجسيمات النانوية وفحص فعالية استخدامها في تبريد الخلايا الشمسية.

هدى البشر

ملخص

مع زيادة الإعتماد على الطاقة المتجددة في الاونة الأخيره زاد الإهتمام بدراسة طرق حفظ الطاقة، وذلك لأن الطاقة المتجددة متذبذبة وغير متوفره طوال الوقت. تُعد أنظمة حفظ الطاقة الكامنة أكثر تقنية واعدة في مجال حفظ الطاقة الحرارية في الوقت الحالي لما لها من مميزات عديدة، أهمها قدرة هذه الأنظمة على حفظ كميات كبيرة من الطاقة الحرارية بدون تغير يذكر في درجة حرارتها. تَستخدم هذه الأنظمة المواد متحولة الحالة الفيزيائية كخزان لحفظ الطاقة الحرارية، ولكن تُعتبر مشكلة التوصيل الحراري الضعيف لهذه المواد أكبرعائق أمام تطوير هذه الأنظمة. لذا في الآونة الأخيرة تكاثفت الجهود من أجل تحسين التوصيل الحراري للمواد متحولة الحالة الفيزيائية بهدف زيادة كفاءتها في تخزين الطاقة، وبالتالي رفع كفاءة النظام. أشارت الدراسات السابقة إلى أن إحدى أفضل الحلول في هذا المجال هو إضافة مواد نانونية إلى المواد متحولة الحالة الفيزيائية بهدف تحسين خواصها الحرارية.

خلال الأبحاث السابقة تمت دراسة إمكانيه استخدام أنواع مختلفة من المواد كمواد متحولة الحالة الفيزيائية وكذلك تمت دراسة تأثير أنواع مختلفة من الإضافات النانونية على خواصها الفيزيائية الحرارية، حيث تم التركيز على دراسة كل إضافة نانونية على حدى. حديثاً تم نشر عدد محدود من الدراسات حول تأثير استخدام أكثر من نوع من الإضافات النانونية معاً (نانو هجين) على الخواص الفيزيائية الحرارية لهذه المواد. بينت الدراسات أن اضافة المواد النانونية يحسن بشكل عام التوصيل الحراري لها.

من ناحية أخرى توجهت الأبحاث إلى دراسة إمكانية استخدام المواد المتحولة الحالة الفيزيائية لتبريد الخلايا الشمسية حيث أن ارتفاع درجة حرارة الخلايا الشمسية لها أضرار سلبية كبيرة على نظام الطاقة الشمسية، تتمثل في انخفاض كبير في كفاءتها. وتعتبر هذه المشكلة احدى أكبر مشاكل أنظمة الطاقة الشمسية التي ما زال يتم العمل والبحث لحلها. كانت نتائج هذه الأبحاث ايجابية حول قدرة استخدام البرافين كمواد متحولة الحالة الفيزيائية لتبريد الخلايا الشمسية.

تعد هذه الدراسة استكمالاً للأبحاث السابقة، حيث تم الأخذ بعين الإعتبار تأثير شكل المواد النانوية المضافة. لذا ركزت هذه الدراسة على إمكانية تحسين التوصيل الحراري للبرافين من خلال إضافة مواد فضة نانونية مختلفة الأشكال إليها (جسيمات فضة نانونية،

أسلاك فضة نانونية، نانو هجين من جسيمات الفضة النانونية وأسلاك الفضة النانونية). وكذلك تم فحص تأثير إضافة هذه المواد النانونية للبرافين بتركيز 0.5% و 1% ، ثم فحص فعالية هذه المادة المحسنة على إدارة وتقليل درجة حرارة الخلايا الشمسية. قمنا بإستخدام برنامج "Solidworks" لانشاء نظام ثلاثي الابعاد ، ثم استخدمنا برنامج " Ansys Fluent " من أجل إجراء محاكاة لدراسة خمس حالات :

- ✓ خلية شمسية تقليدية.
- ✓ خلية شمسية مضاف إليها المواد متحولة الحالة الفيزيائية.
- ✓ خلية شمسية مضاف إليها المواد متحولة الحالة الفيزيائية المحسنة بإضافة جسيمات نانونية إليها.
- ✓ خلية شمسية مضاف إليها المواد متحولة الحالة الفيزيائية المحسنة بإضافة أسلاك نانونية إليها.
- ✓ خلية شمسية مضاف إليها المواد متحولة الحالة الفيزيائية المحسنة بإضافة خليط من جسيمات نانونية وأسلاك نانونية.

قمنا بتعريف الخواص الفيزيائية الحرارية للمواد المحسنة من خلال اقتران يعتمد على درجه الحرارة، حيث تمت كتابتة على شكل كود C ومن ثم إضافته للبرنامج ، ثم قمنا بإجراء المحاكاة ضمن مجموعة من الفرضيات التي أُخذت بعين الإعتبار.

بعد الحصول على النتائج ومقارنتها تم التوصل إلى أن إضافة الأسلاك النانونية بتركيز 1% ، أدى إلى أكبر تحسن في التوصيل الحراري لليرافين، ولكن استخدام المادة المتحولة الحالة الفيزيائية المحسنة بواسطة أسلاك نانونية بتركيز 0.5% لديها أكبر قدرة على إدارة وتقليل درجة حرارة الخلية الشمسية، حيث بلغ انخفاض معدل درجة حرارة الخلية الشمسية 14.9 درجة وارتفعت كفاءتها بمقدار 7.6%. تليها استخدام المواد المحسنة بواسطة جسيمات نانونية بتركيز 1% ، حيث بلغ انخفاض معدل درجة حرارة الخلية الشمسية 12.9 درجة وارتفعت كفاءتها بمقدار 6.6%.

DECLARATION

I declare that the Master Thesis entitled" **Enhancing Thermal Conductivity of Phase Change Materials Using Nanomaterials and its Effectiveness in Cooling Solar Cells**" is my own original work, and herby certify that unless stated, all work contained within this thesis is my own independent research and has not been submitted for the award of any other degree at any institution, except where due acknowledgement is made in the text.

Student Name: Huda Albisher

Signature: Date: 31/8/2023

STATEMENT OF PERMISSION TO USE

In presenting this thesis in partial fulfillment of the requirements for the joint Master's degree in Renewable Energy & Sustainability at Palestine Polytechnic University and Al-Quds University, I agree that the library shall make it available to borrowers under rules of the library.

Brief quotations from this thesis are allowable without special permission, provided that accurate acknowledgement of the source is made.

Permission for extensive quotation from, reproduction, or publication of this thesis may be granted by my main supervisor, or in his absence, by the Dean of Graduate Studies when, in the opinion of either, the proposed use of the material is for scholarly purposes.

Any coping or use of the material in this thesis for financial gain shall not be allowed without my written permission.

Student Name: Huda Albisher

Signature: _____ Date: 31/8/2023

ACKNOWLEDGEMENT

I would like to thank my thesis supervisor Dr. Mostafa Abu Safa for all his time, the support he gave, his advices and his guidance throughout my work.

I would like to thank my family for their continued support.

I also thank my friends for helping and supporting me.

I would like to thank my students for being self-reliant and giving me the chance to finish my thesis.

Table of Content

Abstract……	III
الملخص.....	V
Declaration……	VII
Statement of Permission to Use……..…..……	VIII
Acknowledgement……	IX
List of Abbreviations…….……...…….	XII
List of Figures……..…….……	XIV
List of Tables……	XVI
CHAPTER 1: Introduction	
1.1 Preface …….……	1
1.2 Objectives and Methodology ……	3
1.3 Literature Review ……..….....	4
1.3.1 Adding nanoparticles to phase change materials (0 D) …….	4
1.3.2 Adding nanowires and nanotubes to phase change materials (1D) ……...	5
1.3.3 Adding hybrid nano additives to phase change materials ……..	6
CHAPTER 2: Theory	
2.1 Thermal energy storage …….....	8
2.2 Phase change materials …….……..…	9
2.2.1 Phase change materials types and properties ……..…..…	9
2.2.2 Enhancing thermal conductivity of phase change materials ….	11
2.3 Thermal analysis and heat transfer of PV ……	12
2.4 cooling techniques of PV ……	13
CHAPTER 3: Solar Radiation	
3.1 Solar radiation in Palestine ……	14
3.2 The effect of Solar irradiation on the PV temperature ……..	17
CHAPTER 4: Preparation and Analysis Method	
4.1 Physical system description ……	18
4.2 Numerical model ……..	20

4.3 Numerical simulation ……	24
CHAPTER 5: Results and discussion	
5.1 The effect of temperature on thermophysical properties …….	29
5.2 PV Temperature	
5.2.1 Case I: PV without PCM ……..	31
5.3.2 Case II: PV with PCM ……..	32
5.3.3 Case III: PV With PCM enhanced by nanoparticles ……..…	33
5.3.4 Case IV: PV with PCM enhanced by nanowires …….…….	35
5.3.5 Case V: PV with PCM enhanced by nanohybrid …….	37
CHAPTER 6: Conclusion and Future Work	
6.1 Conclusions …….	39
6.2 Future Work ……...……..	40
REFERENCES …….	41
Appendixes ……...…….	48

List of Abbreviations

PCM	Phase Change Material
PV	Photovoltaic Cell (solar cell)
GW	Gigawatts
CO_2	Carbon dioxide
TES	Thermal Energy Storage
SHS	Sensible Heat Storage
LHS	Latent Heat Storage
TC	Thermal Conductivity
0D	Zero Dimensional
1D	One Dimensional
2D	Two Dimensional
3D	Three Dimensional
NPCM	Nano Phase Change Material
HNPCM	Hybrid Nano Phase Change Material
GNP	Graphene Nanoplatelets
MWCNT	Multi Wall Carbon Nanotubes
THS	Thermochemical Heat Storage
EP	Enthalpy Porosity
UDF	User-Defined Function
ρ	Density (Kg/m^3)
C_p	Specific heat (J/(Kg.K))
T	Temperature
T_m	Melting Temperature
ΔT	Transition Temperature
k	Thermal Conductivity

L	Latent Heat (J/kg)
μ	Viscosity
φ	Volume fraction
s	solid

List of Figures

Figure	Description	Page
Figure 1	(i) Melting process. (ii) Solidification process.	
Figure 2	The PCM's categories.	
Figure 3	The PCM's thermal conductivity enhancing methods.	
Figure 4	The different cooling techniques.	
Figure 5	Global horizontal irradiation (GHI) in West Bank and Gaza.	
Figure 6	Diagram of physical system.	
Figure 7	3D geometry of the PV on Solidworks.	
Figure 8	3D geometry of the PV-PCM on Solidworks.	
Figure 9	Simulation steps.	
Figure 10	The comparison between the thermal conductivity of PCM, NPCM and HNPCM.	
Figure 11	The comparison between the thermal conductivity and the latent heat of PCM, NPCM and HNPCM	
Figure 12	The temperature of PV during two hours.	
Figure 13	(i) The temperature of PV−PCM during two hours. (ii) The comparison between the temperature of PV with PCM and without PCM.	
Figure 14	The comparison between the temperature of PV−NPCM (φ=0.5% nanoparticles) and PV without PCM.	
Figure 15	The comparison between the temperature of PV−NPCM (φ=1% nanoparticles) and PV without PCM.	
Figure 16	The comparison between the temperature of PV−NPCM (φ=0.5% nanowires) and PV without PCM.	
Figure 17	The comparison between the temperature of PV−NPCM (φ=1% nanowires) and PV without PCM.	
Figure 18	The comparison between the temperature of PV−HNPCM (φ=0.5%) and PV without PCM.	

Figure 19 The comparison between the temperature of PV−HNPCM (φ=1%) and PV without PCM.

List of Tables

Table	Description	Page
Table 1	Monthly of GHI in Hebron city	
Table 2	Thermo-physical properties and thickness of PV module layers.	
Table 3	Thermo-physical properties of PCM (RT25HC) and Ag	

CHAPTER 1: Introduction

1.1 Preface

In recent decades, population growth and economic growth have increased, which led to an increase in energy demand. Primary energy consumption rose by 2.8% and 1.3% in the years 2018 and 2019 respectively [bp report, 2020]. On the other side, in 2020, primary energy consumption declined by 4.5%, which is the largest drop since 1945, this is due to the impact of COVID-19 on energy markets [bp report, 2021]. After COVID-19 subsides, the energy consumption is predicted to rise until 2050 as population and economic growth [AEO2022 Narrative, 2022]. Carbon dioxide (CO_2) emissions rise along with an increase in energy usage. In 2021, CO_2 emissions related to global energy have been raised by 1.2 billion tons. The raise in electricity demand along with a growth in the usage of coal are responsible for nearly 30% of this increase [IEA report, 2021]. This negatively affects the environment and the global climate.

Renewable energy is the realistic choice to cover the rise in energy demand and at the same time to not increase CO_2 emissions. Renewables were responsible for 38% of global installed capacity by the end of 2021. In 2021, the world aggregated almost 257 Gigawatts (GW) of renewables, also Solar power alone was responsible for more than half of the renewable installations which was recorded 133 GW, followed by 93 GW of the wind energy overall [IRENA, 2022]. However, renewable energy sources are intermittent, for example, solar energy is not available at night. Thus, storing the excess energy during the time when it is available and using it at the other time when it is not available is the solution to ensure that the system works all day.

Recently, the storage of energy mainly depends on Li-ion batteries, in spite of the environmental pollution that such batteries caused [Gadhave et al., 2021]. Another method of energy storage that has been introduced in recent decades and has attracted many researchers is the thermal energy storage (TES). There are three types of TES techniques: latent heat storage (LHS), sensible heat storage (SHS) and thermochemical heat storage [Gadhave et al., 2021; Tao and He, 2018]. In LHS system, phase change material (PCM) is employed as a thermal energy storage medium. PCM is any material that can store or release thermal energy through melting and solidification process. PCM store energy when it transforms from a solid state to a liquid state (melting process), and this material

releases stored energy when it changes from a liquid state to a solid state (solidification process). [Tao and He, 2018; Tofani and Tiari, 2021].

Presently, LHS is the most promising technique and has many applications due to its many features, like; large energy storage density, melting and solidification cyclic at constant temperature, large array of PCMs and Small volume [Tao and He, 2018; Gadhave et al., 2021; Tofani and Tiari, 2021; W. Liu et al., 2021]. There are many articles that have been published on the applications of LHS systems and PCMs types and their properties. The major drawback of LHS is low thermal conductivity of PCM [Tao and He, 2018; Tofani and Tiari, 2021; W. Liu et al., 2021; Sharma et al., 2021], which ranges between 0.2 W $m^{-1}K^{-1}$ and 0.4 W $m^{-1}K^{-1}$ [Sharma et al., 2021].

Low Thermal Conductivity (TC) negatively affects the performance of PCMs, which results in a low heat transfer rate and very long time of charging and discharging thermal energy (melting and solidification process) [Tofani and Tiari, 2021; Tao and He, 2018]. Enhancing the TC of PCM maximizes the efficiency of the system. Therefore, many researchers aimed to enhance the TC of PCM. Most common techniques include of fin, metallic foam and nanomaterial additives [Yang et al., 2020]. Improving the TC of PCM is positively reflected on all their applications, which includes improving thermal management of photovoltaic cells (PV) using PCMs.

The raise of PV operating temperature negatively influences its electrical efficiency and its life span. Moreover, it rises its payback period [Preet, 2021]. When the PV temperature increases above the range of 25-27 °C, the electrical energy starts to drop because of heat expansion in the system [Hassan et al., 2020]. Previous study pointed out that temperature rising leads to decrease the PV electrical output by 0.4-0.65% per degree [Breeze, 2016; Sharma et al., 2021]. Therefore, the PV thermal management system is necessary to regulate the PV temperature in a normal operating temperature range thus improve their efficiency.

In this thesis, we present a study about using silver nano additives to enhance the thermal conductivity of paraffin as a PCM. Followed by an analysis of the ability of this improved material to decrease the PV temperature thus improving its efficiency. Ansys fluent software is used to simulate a 3D system. This thesis contains five chapters; the first chapter includes an introduction and literature review. The second chapter presents the theory of the thesis. The third chapter explains the

method applied to achieve the aim of the thesis. The fourth chapter discusses the results that are obtained, and the last chapter shows the conclusions and future work.

1.2 Objectives and Methodology

*** Objectives:**

1) To present a study on improving the efficiency of solar cells through cooling using enhanced PCM by adding nanomaterials.

2) To investigate the impact of volume fraction and shape of the added nanomaterials on the thermo-physical properties of PCM (paraffin).

3) To make a comparison in the performance of enhanced PCM using either nanoparticles, nanowires, or hybrid nanomaterials in cooling the PV and enhancing its efficiency, and to conclude which one is the most effective approach among them.

*** Methodology:**

1) Reviewing previous studies which related to enhancing the efficiency of PV through cooling using PCM enhanced by adding nanomaterials.

2) Analyzing solar irradiation in Palestine.

3) Collecting data related to the composition of PV module and the thermo-physical properties of PV layers.

4) Gathering data about thermo-physical properties for both PCM and nanomaterials that we used.

5) Simulating PV system and PV-PCM system using “Ansys fluent” software.

6) Simulating PV with PCM enhanced by nanoparticles, nanowires and nanohybrid.

7) Presenting the results, conclusions and comparing outcomes.

1.3 Literature Review

The nanomaterials added to PCM in previous studies can be divided, based on their shape, into several types, first zero dimensional (0D) which is a nanoparticle, one dimensional (1D) such as nanotubes and nanowires, two dimensional (2D) as nanoplates and three dimensional. If more than one type of nanomaterial have been used together, this case is called nanohybrid.

1.3.1 Adding nanoparticles to phase change materials (0 D)

Siahkamari et al, have accomplished an experimental examination of using PCM in PV cooling. In their experiment, they used sheep's grease as a PCM and then enhanced it by adding CuO nanoparticles to the PCM. Their results indicated that using improved sheep's grease by adding nanoparticles led to decline in the average temperature surface of PV by 14.2 °C compared to the cases of using pure sheep's grease, and the maximum produced power is risen by about 24.6% to 26.2% [Siahkamari et al., 2019]. Sharma et al, also have worked out an experimental study. In their study, they used two types of nanoparticles (Al_2O_3 and CuO) at different volume concentrations to enhance paraffin TC. This study came out that the thermal conductivity rises when any of the temperature or the nanoparticles concentration increase. The Maximum enhancement was 19 % when PCM has been improved by CuO at 70°C [Sharma et al., 2018].

Another experimental study was conducted by Nada et al, in which they used Paraffin (RT56) as PCM with Al_2O_3 nanoparticles. Results demonstrated that using PCM with nanoparticles increases the ability to manage and reduce PV temperature, hence increasing its efficiency. For pure PCM and PCM enhanced by nanoparticles, the PV temperature decreased by 8.1°C and 10.6°C, respectively, and its efficiency incremented by 5.7% and 13.2% [Nada et al., 2018]. Salem et al, experimentally found that PV temperature dropped by 14.5 °C when using Calcium chloride hexahydrate as PCM with Al_2O_3 nanoparticles. Their outcomes showed that electrical efficiency and thermal efficiency were improved by 22.7% and 78% respectively. The Maximum rise in energy efficiency was 52.3% [Salem et al., 2019]. Al-Waeli et al, presented experimentally the impact of using nano-PCM on the photovoltaic thermal system (paraffin waxes as PCM and SiC as nanoparticles). They found out that the maximum minimizing of PV temperature's value was 17°C, and this decrease in temperature

caused an enhance in the electrical efficiency of PV from 7.1% to 13.7%. Besides, the system improved and its thermal efficiency reached to 72% [Al-Waeli et al., 2017].

Aurangzeb et al, experimentally proved that using nanoparticles in PCM enhanced the heat transfer. They used two types of PCMs (RT26 and coconut oil) and two types of nanoparticles (Fe_3O_4 and Al_2O_3). The results denoted that the maximum improvement in heat transfer when using RT26 enhanced by Fe_3O_4 and Al_2O_3 reached up to 20.01% and 36.68% respectively. Moreover, the maximum improvement in heat transfer when using coconut oil enhanced by Fe_3O_4 and Al_2O_3 is up to 8.83% and 14.84% respectively [Aurangzeb et al., 2022].

In addition to the many experimental researches, which studied improving PCMs by adding nanoparticles, there are some numerical studies in this field. The performance of LHS devices integrated with enhanced PCM by Al_2O_3 nanoparticles was numerically simulated by Akhmetov et al. PCM is paraffin waxes. The results demonstrated that using nano-PCM improved the ability of heat transfer and thus led to enhancing the charging and discharging efficiency. The full charging time decreased by 57 min and 106 min when using enhanced PCM with 2 wt% and 4 wt% nanoparticles respectively. Additionally, the full discharging time declined by 32 min and 74 min [Akhmetov et al., 2019]. Zarma et al, numerically studied the effect of adding nanoparticles to enhance the TC of PCM. They used four different PCMs namely; pure salt hydrate, eutectic of capric –palmitic acid, n- octadecane paraffin and dodecanol. Oxide nanoparticles (CuO) which been used to enhance the four PCMs. The results pointed out that thermal conductivity of nano-PCM is greater than the pure PCMs [Zarma et al., 2017]. A 2D numerical model was developed by Sushobhan and Kar to simulate the melting process of nano-PCM (n-octadecane with CuO nanoparticles). They concluded that TC improved compared with conventional PCM, thus heat transfer became higher and the melting rate became fast, as a result, the melting time decreased [Sushobhan and Kar, 2017].

1.3.2 Adding nanowires and nanotubes to phase change materials (1D)

Liang et al, experimentally checked the impact of adding MnO_2 nanowires and nanotubes in PCM, which was palmitic acid. They observed that the TC of nano-PCM (NPCM) was greatly improved by the integration of MnO_2 nanotubes and nanowires with a maximum value of 377.16% compared to pure palmitic acid. The NPCM also showed an excellent thermal stability of recyclability. Only 2.8% of the latent heat was lost after 100 melting / solidification cycles. [Liang et al., 2018]. Karaipekli et

al, detected that adding the Carbon nanotubes in mass fraction of 1 wt%, caused a considerable rise in the TC of the perlite/paraffin composite (when it used as a PCM) up to 113.3%. And the total melting and freezing period were reduced appreciably due to the TC enhancement [Karaipekli et al, 2017].

In addition, the impact of adding multiwalled carbon nanotubes was experimentally studied on the thermal properties of lauryl alcohol as a PCM. The results indicated that the addition of multiwalled carbon nanotubes significantly rose the TC of lauryl alcohol, and the maximum increase in the TC of lauryl alcohol happened when adding 5 wt% of multiwalled carbon nanotubes to it [Chinnasamy and Cho, 2022]. Moreover, Bocharov et al indicated that adding carbon nanotubes to paraffin at 10 wt% leads to enhance the TC by about 100% [Bocharov et al., 2020].

1.3.3 Adding hybrid nano additives to phase change materials

Pasupathi et al, showed an experimental study of the thermophysical properties of paraffin under the effect of different mass fractions of hybrid nanoparticles which were SiO_2 and CeO_2 nanoparticles (50%:50%). The results pointed out that the TC of the paraffin was enhanced by about 165.56% when adding nanohybrid in it. Using 1wt% nanohybrid, gave a better result comparing to the result for higher mass fractions, and this result caused an increase in the TC without too much reduction in the latent heat of the paraffin [Pasupathi et al., 2020]. Another experiment was conducted by Qu et al to study the impact of adding nanohybrid on the TC of Paraffin-HDPE SSPCM. This nanohybrid consist of two types of carbon nano additives, which were expanded graphite multiwalled carbon nanotube (nano1) and expanded graphite carbon nanofiber (nano2). They tested five mass ratios of nano1:nano2, the largest TC was obtained when the mass ratio was 4:1. The TC reached 1.36 $Wm^{-1}\cdot K^{-1}$ with an improvement of 444% compared with using the pure paraffin [Qu, Wang, Zhou and Tian, 2020].

A numerical study concentrated on thermal performance of the hybrid nano-PCM (HNPCM). The effect of adding hybrid nanoparticles TiO2–CuO (50%–50%) was studied at different small mass fractions on the TC. The outcomes demonstrated that both TC and density of PCM were improved by adding hybrid nanoparticles, but at the same time, it reduced the stored energy. When nanohybrid was added at 1 mass %, the average charging time improved by 27.33 %, but the stored energy was reduced by 3.88%. Moreover, the discharging time was decreased by 30.52% [BENLEKKAM and

NEHARI, 2022]. Another nanohybrid included Al nanoparticle and coated C was tested experimentally to enhance the TC of sodium sulfate decahydrate which was used as PCM. It was observed that adding about 3 wt% of this nanohybrid to PCM led to an increase in TC by 26.41% (at 30 °C) and also led to a decrease in the solidification latent heat enthalpy by 5.13% [X. Liu et al., 2021]. Aslfattahi et al used the MATLAB program to survey the ability of using hybrid Graphene-Silver (Gr-Ag) nanomaterial to enhance the TC of paraffin. They found that adding nanohybrid at 0.3% mass concentration to PCM leads to enhancing the specific heat capacity about 40%. Moreover, the highest TC increment is about 11%. In addition, the thermal efficiency incremented by 4.16% compared with the case of using pure PCM [Aslfattahi et al., 2020].

An experimental study was done to examine the thermal properties of paraffin (RT-28HC) enhanced by nanomaterials at 1wt%. In this experiment, four types of nanomaterials were used, graphene nanoplatelets (GNP), multiwall carbon nanotubes (MWCNT), aluminum oxide and copper oxide. The results showed that the HNPCM with GNP-MWCNT at mass percentage ratio of 75%-25% had the highest TC compared with the case of using one type of nanomaterial [Arshad, Jabbal and Yan, 2020]. Ibrahim et al, studied the stability and the TC of Iraqi paraffin when dispersing hybrid nanoparticles TiO_2–MgO (50%:50%) in it. The TC of HNPCM was enhanced and the highest obtained value was 24.92%. Furthermore, the HNPCM demonstrated excellent stability for more than 90 days. Hence, the study concluded that using Iraqi paraffin enhanced by nanohybrid suits solar energy applications [Ibrahim et al., 2022].

Zou et al conducted another experimental survey about the possibility of enhancing the TC of PCM (which is one of the paraffin types) by using graphene and carbon nanotubes as nano additives. Outcomes illustrated that HNPCM with MWCNT-graphene at mass ratio of 3-7 gave the best improvement in heat transfer. The TC was incremented by 31.8%, 55.4% and 124% compared with the case of using PCM with graphene only, PCM with MWCNT only and pure PCM respectively [Zou et al., 2018].

Through our review of previous studies, we found that they focused on studying each nano-additive separately. On the other hand, few published studies discussed the effect of using more than one type of nano-additives together (nanohybrid). Our thesis is a continuation of previous studies, as we took into consideration the effect of added nanomaterials' shape, and we focused on the possibility of

enhancing the TC of paraffin by adding different shapes (nanoparticles, nanowires and nanohybrid) of silver nanomaterials.

CHAPTER 2: Theory

In recent decades, there has been a great reliance on renewable energy, particularly, the solar energy, which requires more attention and work to increase the efficiency of solar energy systems, furthermore, study and develop energy storage methods. Because the renewable energy is intermittent and not available all the time. In this thesis, work has been done to improve the efficiency of the PV system by cooling it using one of the thermal energy storage methods.

In this chapter, we focus on explaining the thesis theory. This chapter is divided into four sections. The first section concentrates on explaining the thermal energy storage systems and their types. While the second section focuses on the PCM's types and the different methods that were used to improve their thermophysical properties. The third section includes a thermal analysis and heat transfer of PV. Finally, the fourth section contains of the cooling techniques of PV.

2.1 Thermal energy storage

One of the energy storage methods is thermal energy storage (TES) that researchers recently pay attention to. The TES is a technology that absorbs the thermal energy and stores it by heating a specific material (a storage medium) [Sarbu & Sebarchievici, 2018]. TES has three groups; Latent Heat Storage (LHS), Sensible Heat Storage (SHS) and Thermochemical Heat Storage (THS) [Gadhave et al., 2021; Tao and He, 2018; Sarbu & Sebarchievici, 2018; Alva et al., 2018]. The thermal energy in SHS is absorbed and saved by increasing the storage material's temperature without changing its physical phase. This energy is released when the material's temperature is decreased. The storage material may be liquid or solid. This method has advantages and at the same time several drawbacks, such as low storage capacity and a large volume requirements [Enescu et al., 2020].

In THS, the thermal energy is stored and released through a reversible chemical reaction. Although this technology has a high thermal energy storage density, it faces many challenges represented by the high cost, toxicity, low system life [Enescu et al., 2020].

In LHS, the thermal energy is stored and released through a phase change process of materials. The materials used in LHS systems are called PCM. The thermal energy in these systems is absorbed and stored through the transition state of PCM from solid phase to liquid phase (melting process), and when PCM changes from liquid phase to solid phase (solidification process), this energy is released. Which means that the charging and discharging cycle in these systems is melting and solidification processes [Tao and He, 2018; Tofani and Tiari, 2021; Enescu et al., 2020]. Comparing the three types of TES, the LHS type is the most promising method for TES thanks to its many features, which is better than the other two types. Its features are melting and solidification cyclic occurs at almost constant temperature, large energy storage density, small volume and large array of PCMs [Tao and He, 2018; Gadhave et al., 2021; Tofani and Tiari, 2021; W. Liu et al., 2021; Sarbu & Sebarchievici, 2018; Ma et al., 2019].

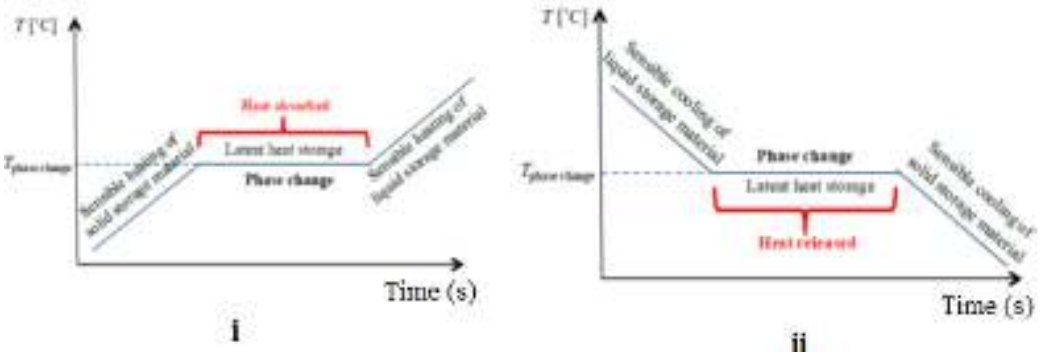

Figure 1: (i) Melting process. (ii) Solidification process.

2.2 Phase change materials

In previous studies, different types of materials were used as PCM. The materials that are used as PCMs should have some characteristics such as chemical stability, high density, high TC, high latent heat, nonreactive, long life cycle and minimum or no change in volume after freezing or melting [Sharma et al., 2021; Ma et al., 2019]. Moreover, safe, eco-friendly and effectiveness of cost [Ma et al., 2019].

2.2.1 Phase change materials types and properties

The types of PCM are classified into three main groups; inorganic PCM, organic PCM and eutectic PCM [Sharma et al., 2021; Irfan Lone & Jilte, 2021; Preet, 2021]. Organic PCMs are classified as paraffin and nonparaffin [Preet, 2021; Irfan Lone & Jilte, 2021]. Organic PCM has many features; however, its low TC is a major drawback [Sharma et al., 2021; Preet, 2021; W. Liu et al., 2021; Tofani and Tiari, 2021]. The TC of organic PCM is low and the range of its value is between 0.18 to 0.24 W $m^{-1}K^{-1}$, which negatively affects the heat transfer rate in the PCM. Thus, it limits its efficiency in cooling PV during daytime. In addition, it has a negative impact on releasing this heat to surrounding at night [Sharma et al., 2021].

Inorganic PCM includes salt hydrates and metals. Inorganic PCMs have higher TC than organic PCMs, and many other advantages. Nevertheless, it has many disadvantages which are summarized in previous articles [Sharma et al., 2021; Preet, 2021; Seto et al., 2021; Irfan Lone & Jilte, 2021; Sarbu & Sebarchievici, 2018], therefore, it is difficult to deal with it. Eutectic is a mixture of at least two types of PCMs, which can be inorganic–inorganic, organic–organic and organic–inorganic [Ma et al., 2019; Sharma et al., 2021; Preet, 2021]. The aim of mixing two or more types of PCMs is to attain the required properties [Ma et al., 2019].

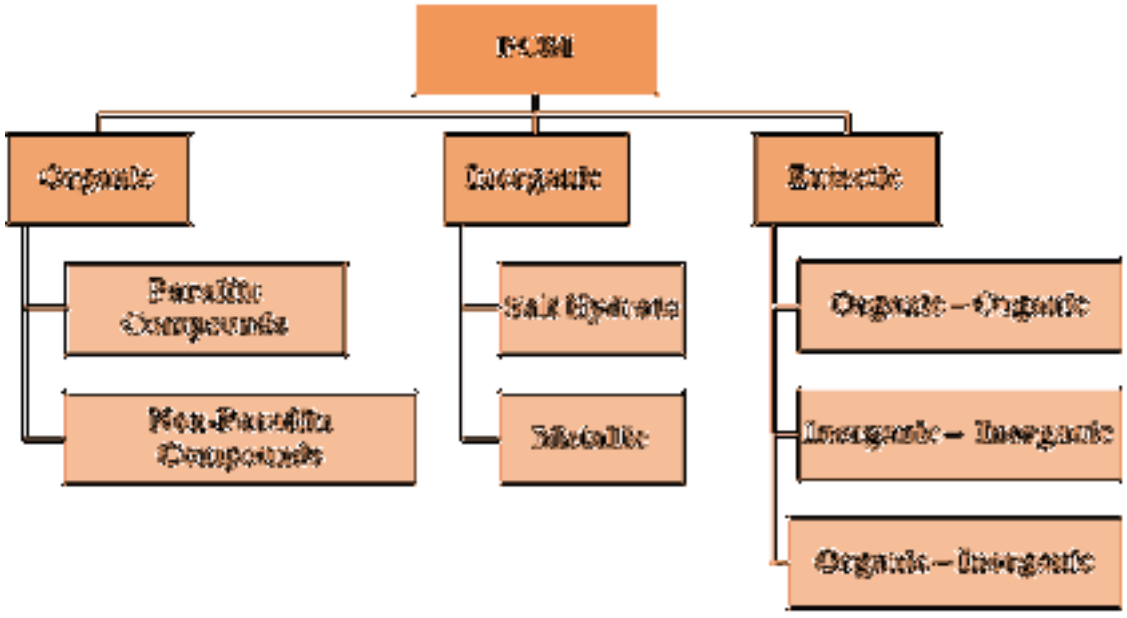

Figure 2: The PCM's categories [Irfan Lone & Jilte, 2021].

2.2.2 Enhancing thermal conductivity of phase change materials

The low TC affects the performance of PCM negatively; moreover, it minimizes their practical application and energy utilization efficiency greatly [Cheng et al., 2021]. The low TC weakens the rate of the heat transfer, so the time of charging and discharging thermal energy (melting and solidification) becomes very long [Tofani and Tiari, 2021; Tao and He, 2018; Alva et al., 2018]. According to previous studies, various efficient techniques have been mentioned to rise the TC of PCM. The most popular techniques are; addition fin, metallic foam, adding nanomaterial inside PCM and encapsulation of PCM [Yang et al., 2020; Qureshi et al., 2018].

The application of metallic foam or metallic fin to enhance TC of PCM leads to increase the PCM's weight and the PCM holders' fabrication cost. These two problems can largely be overcome by adding nanomaterials to the PCM. The TC of PCM is enhanced by adding nanomaterials with high TC in it, [Yang et al., 2020]. The nanomaterials additives are divided into; 0D additives (metal and metal oxide nanoparticles), 1D additives (nanowires and nanotubes), 2D nanoadditives (nanosheets) and 3D nanoadditives [Cheng et al., 2021; W. Liu et al., 2021].

Figure 3: The PCM's thermal conductivity enhancing methods.

2.3 Thermal analysis and heat transfer of PV

The PV performance relies on a number of operational, environmental and physical conditions; also, it depends on design constraints. For a typical PV, the percentage of the solar radiation that converted into electricity ranges from 5–25% [Kant et al., 2016a]. Then, the remaining absorbed energy converts into heat, which causes a rise in the PV temperature [Sharma et al., 2021; Kant et al., 2016b]. The current value, which is resulted by PV, has slightly risen when the temperature of the cell becomes greater, but the voltage is greatly dropped. Consequently, this lead to a drop in the generated maximum power [Popovici et al., 2016].

The raise of the PV operating temperature negatively impacts its life span and its electrical performance. Moreover, it rises its payback period [Preet, 2021]. When the temperature of PV increases above 25-27 °C, the electrical energy begins to decline due to the rise in the system's temperature [Hassan et al., 2020]. It is reported that temperature rising leads to decrease the PV electrical output by 0.4-0.65% per degree [Breeze, 2016; Sharma et al., 2021]. So, the thermal regulation of PV is crucial to manage the PV's temperature in a normal operating temperature range to get the maximum benefit from the solar panels. Recently, the use of PCM in PV for thermal regulation has attracted wide interest in this field, since the hybrid PV-PCM method can obtain greater photoelectric conversion efficiency and the PCM's stored thermal energy can be extracted for various uses. [Ma et al., 2019].

The PV efficiency depends on its temperature. The PV temperature depends on the heat transfers, which happened through conduction, convection and radiation. The conduction is a way of heat transfer in the solid parts of the PV-PCM system, which contains five layers of PV, Aluminum (Al) box added behind the PV and PCM in solid state. The heat is transferred from the PV or PV-PCM system to the environment by thermal radiation and convection from front and rear surface of the system. The effective radiation that is released from the PV’s front surface and aluminum's back surface mainly depends on the temperature of both surfaces, the surface emissivity, the surrounding

temperature and the tilt angle. The heat transfers via convection from the PV to the surrounding through natural convection and forced convection. Losing heat via forced convection requires external force such as wind force. In the melted PCM, the heat transfers by convection and conduction methods [Preet, 2021; Kant et al., 2016b]. Generally, the good heat transfer rate has positive impact on minimizing the PV temperature.

2.4 PV cooling techniques

The PV's working temperature is a crucial factor that influences the PV's performance, so the PV should be cooled to increase its efficiency. The cooling techniques of PV are usually classified into; active cooling techniques and passive cooling techniques [Ma et al., 2019; Sharma et al., 2021; Kant et al., 2016b].

The Active cooling method is a method that requires an external mechanical device to pump the required air or water to cool the PV. The PV performance can be improved by this strategy, but it requires an external source. This power is subtracted from the energy produced by the PV, which minimizes the PV's net output power. Moreover, it needs high initial and maintenance cost [Sharaf et al., 2022]. The Passive cooling method relies on nature to cool the medium, which is highly based on; PCMs, liquid (nanofluids, etc.), air and the sky radiation [Ma et al., 2019]. The passive cooling method is simple, easy and low cost, at the same time it has low heat transfer rate, so the PV performance is not highly enhanced [Sharaf et al., 2022].

The PCM cooling method, is one of the passive cooling technologies. It is regarded as one of the effective upcoming techniques for PV cooling. Because of that, the PCM absorbs a great amount of heat without obvious rise in its temperature, and there are no moving parts or external energy sources required for this method. As a result, PV-PCM systems typically offer better cooling performance than other passive cooling methods such as natural air and water cooling; also, it requires less maintenance cost than active cooling methods. [Ma et al., 2019]. Because of the low TC of the PCM, the PCM's efficiency is reduced. Therefore, improving the cooling performance requires that the TC of the PCM should be optimized by adding another component to it [Sharaf et al., 2022] such as nanomaterials.

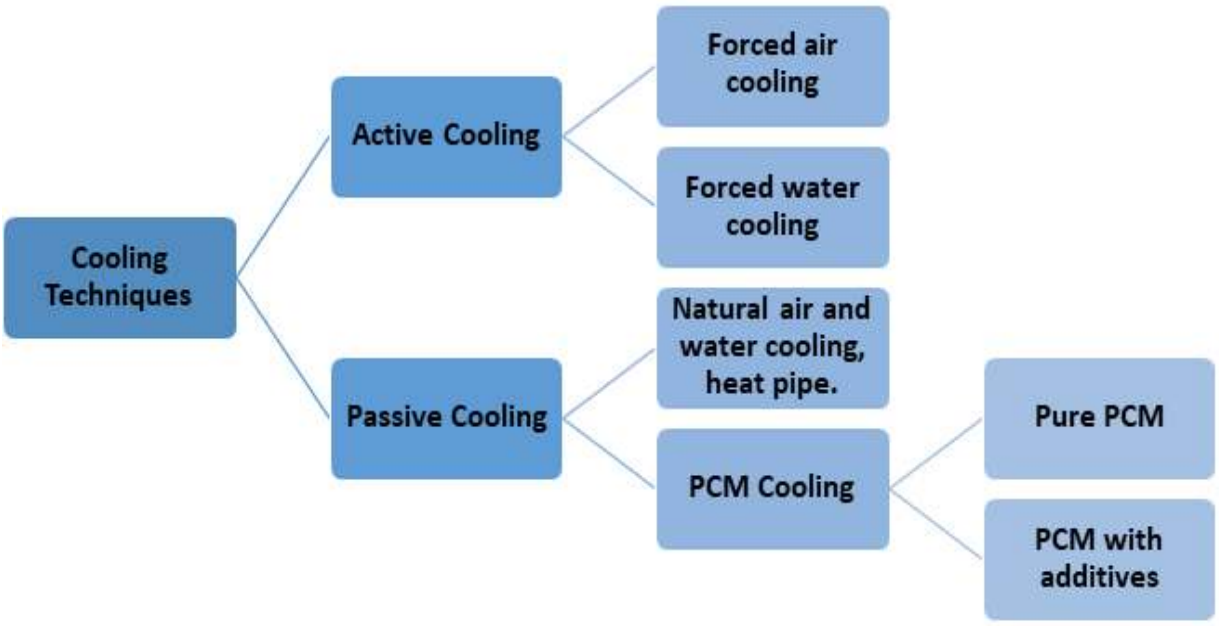

Figure 4: The different cooling techniques of PV.

Chapter 3: Solar radiation

3.1 Solar radiation in Palestine

The Middle East region is renowned for its abundant solar radiation levels, positioning it as a region with vast solar energy potential. Palestine, as one of the Middle East's countries, so it benefits from this potential. Palestine is boasting by having approximately 3000 sunshine hours per year. It also particularizes with a high annual average of solar radiation, reaching 5.4 kWh/m^2/day on a horizontal surface. The solar radiation on a horizontal surface varies throughout the year, ranging from 2.63 kWh/m^2/day in December to 8.4 kWh/m^2/day in June [Juaidi et al., 2016].

In Palestinian regions, there is a variation in the irradiation levels, and this lead to classifying Palestine into three distinct areas. The areas with the highest irradiation levels are mostly situated in the middle and southern regions. Meanwhile, the areas with medium irradiation cover the Jordan

Valley and the northern hilly regions of Palestine. Lastly, the areas with low irradiation, which represented by the yellow color, are widespread in the northern areas of the West Bank [Rabi and Ghanem, 2016].

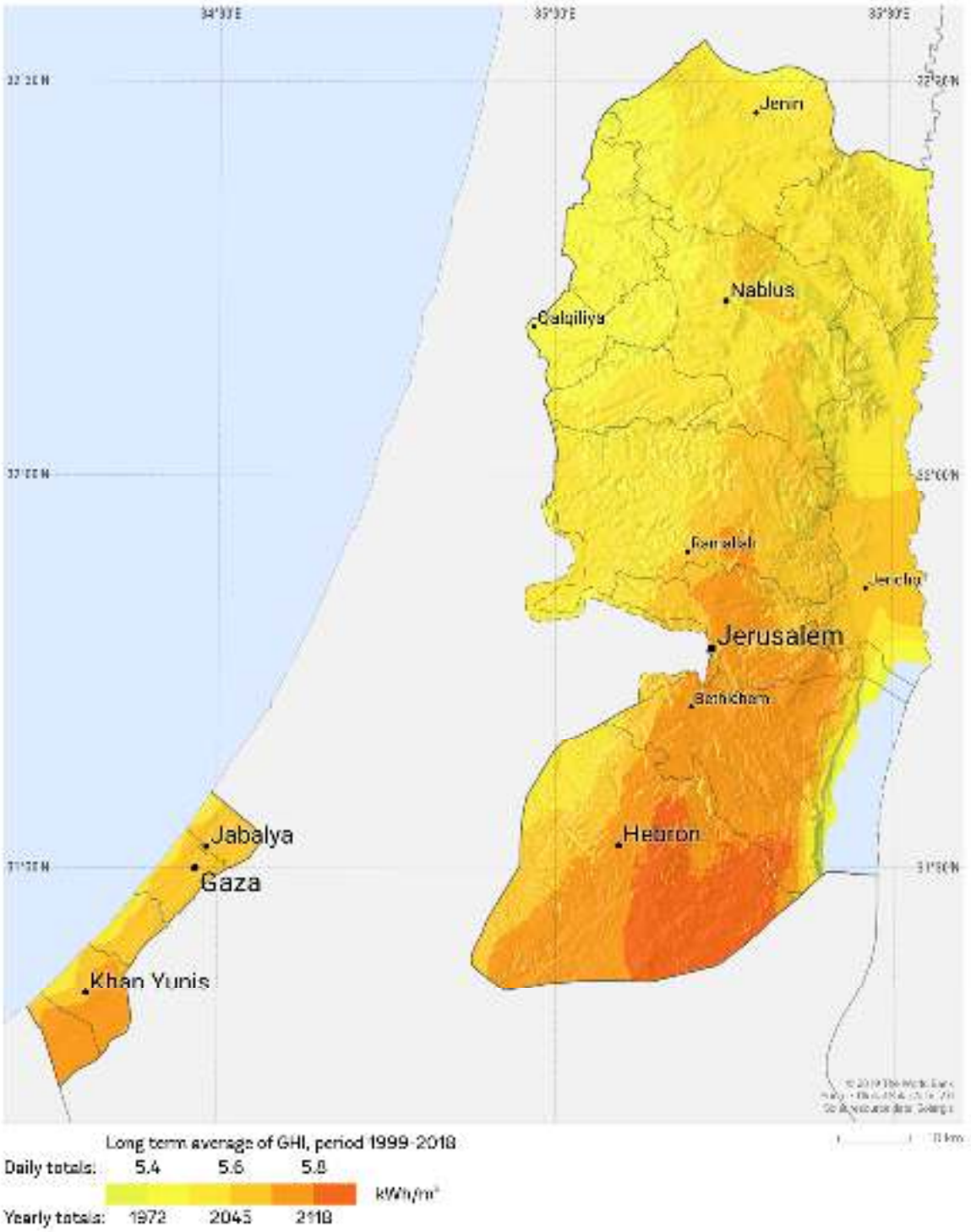

Figure 5: Global horizontal irradiation (GHI) in West Bank and Gaza [GLOBAL SOLAR ATLAS, 2019].

Hebron city is located in an area, which is characterized by high levels of irradiation. The monthly Global Horizontal Irradiance (GHI) data for Hebron city are presented in the table below. These data were collected from the Atlas of Solar Resources of the State of Palestine in 2014 [Rabi and Ghanem, 2016]. The highest GHI values were recorded in June and July, and these values reached 263 kWh/m^2. Conversely, the lowest GHI value was observed in January and it measured 76 kWh/m^2.

Month	**GHI (kWh/m^2)**		
	Min	Max	Average
January	76	104	91
February	86	121	104
March	127	183	157
April	162	215	187
May	214	254	237
June	244	263	256
July	248	263	256
August	231	240	236
September	176	200	190
October	132	161	147
November	78	124	107
December	79	102	90

Table 1: Monthly of GHI in Hebron city [Rabi and Ghanem, 2016].

In a study conducted by Alsamamra, it was observed over a 4 years period (from January 2007 to December 2010) that the highest values of sunshine duration in Hebron occurred in June and July, with an average duration 11.86 hours and 12.05 hours, respectively. Conversely, the lowest sunshine

duration was recorded in December, with an average duration 5.14 hours [Alsamamra, 2013]. Additionally, the highest solar radiation in Hebron was reported 7.51 kWh/m2/day in June of 2010, while the lowest solar radiation occurred in January [Juaidi et al., 2016].

According to the data from National Solar Radiation Database (NSRDB), the GHI values were obtained for every hour in every day in the years 2017, 2018 and 2019 in Hebron. The highest and lowest daily GHI values occurred in 2017, reaching 8989 W/m²/day (in June) and 209 W/m²/day, respectively. The average daily irradiation for the years 2017, 2018 and 2019 was 5670 W/m²/day, 5463 W/m²/day, and 5565 W/m²/day, respectively [NSRDB]. Additionally, when examining the hourly GHI values, it was observed that from about the second half of May until the beginning of August, we have solar radiation of approximately 1000 W/m^2 which extending almost for two consecutive hours at noon. Since in our study, we assumed a constant solar radiation value of 1000 W/m^2 and conducted the simulation for two consecutive hours, Hebron would be a suitable location to conduct this study as it has a favorable solar radiation condition, which aligning with the study's assumptions. Certainly, if the study is conducted in the areas that experience significantly different solar radiation than the assumptions considered in the study, and that may yield to different results.

3.2 The effect of Solar irradiation on the PV temperature

Solar irradiation plays crucial role in determining the temperature of PV cells. The higher solar radiation levels result an increased in PV temperatures [Zhou et al., 2015; Maan et al., 2018]. The elevation of PV temperature has been recognized as a primary factor that lead to decline PV's output. Multiple studies have examined this relationship and have reported consistent findings. For example, Nasrin et al. conducted a numerical simulation on photovoltaic thermal system, which observed that for each increment of 100 W/m^2 in solar irradiation, the solar cell temperature increased by approximately 1.85°C. Their study encompassed an operating irradiation that ranges between 1000 to 3000 W/m^2 [Nasrin et al., 2017]. Similarly, Bahaidarah et al. conducted numerical and experimental analysis of a PV-water cooled hybrid system with an operating irradiation range between 240 to 979 W/m^2. They found that for every increase of 100 W/m^2 in irradiation level, the PV temperature increased by approximately 1.9°C [Bahaidarah et al., 2013].

In another study by Rahman et al., with an operating irradiation range between 312 to 995 W/m^2, it was observed that the PV temperature increased by around 3.82°C for each increase of 100 W/m^2 in irradiation level [Rahman et al., 2017]. All these studies demonstrate a consistent trend: as solar irradiation levels increase; PV temperatures rise accordingly.

CHAPTER 4: Preparation and Analysis Method

This chapter includes three sections. The first one describes the physical model that was used to study the impact of adding nanoparticles, nanowires and nanohybrid on PCM in order to manage and reduce the PV's temperature. The second section explains the numerical model and shows the mathematical equations that describe the PCM's thermo-physical properties. In the third section, the work steps that were accomplished on the Ansys Fluent will be explained, and the assumptions and limitations were taken into consideration in the simulation will be deconcentrated.

4.1 Physical system description

PV module contains five layers with different thermo-physical and optical properties [Kant et al., 2016a], which are given on the tables below. In the first case, the prevailing PV panel is used for thermal analysis without any additives. In the second case, an aluminum box filled with paraffin PCM has been added below the PV module to reduce PV temperature as shown in figure 6 [Kant et al., 2016b]. The thermo-physical features of the aluminum box that used in the second case and PCM are also given on the tables below.

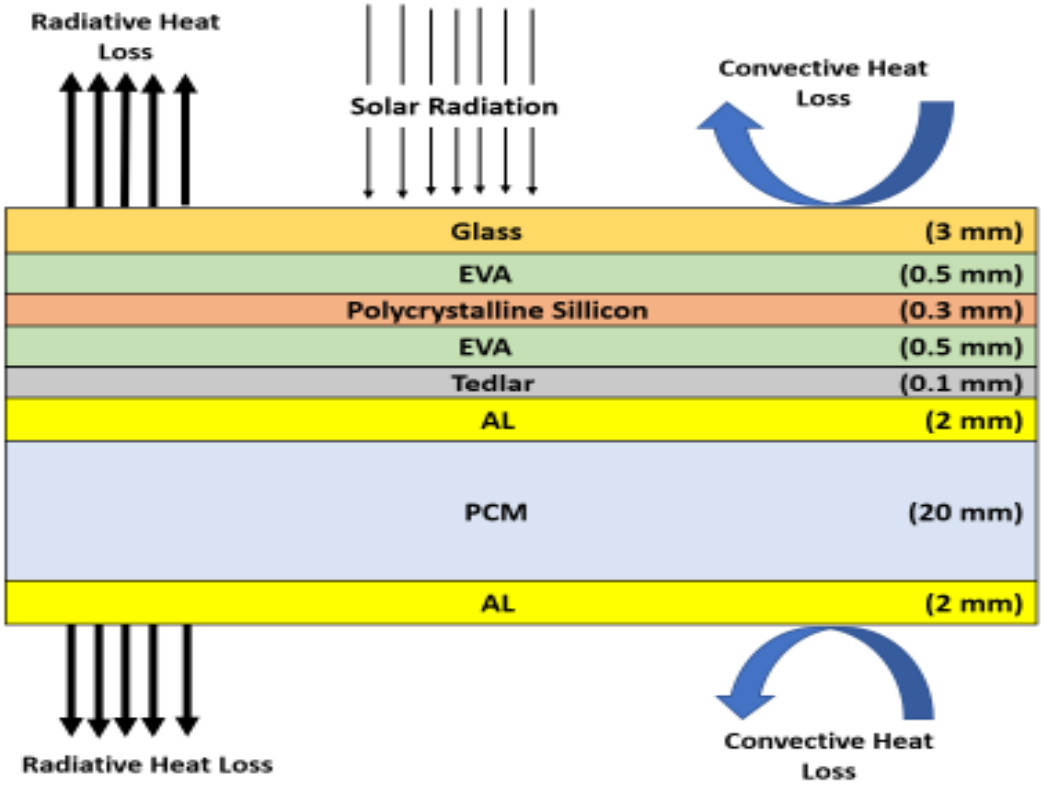

Figure 6: diagram of physical system.

Table 2: Thermo-physical properties and thickness of PV module layers [Charles Divyateja et al., 2021]

Material	Density (kg/m^3)	Specific heat (J/kg. K)	Thermal conductivity (W/m. K)	Thickness (mm)
Glass	3000	500	1.8	3
EVA	960	2090	0.35	0.5
Silicon	2330	677	148	0.3
Tedlar	1200	1250	0.2	0.1
AL	2675	903	211	2

In the remaining three cases, PCM was enhanced with silver nanomaterial. In the third case, it was enhanced by silver (Ag) nanoparticles. In the fourth case, it was enhanced by Ag nanowires. However, in the last case, it was enhanced by a hybrid of Ag nanoparticles and Ag nanowires with a percentage of (50%-50%). In these last three cases, two different volume fractions of Ag

nanomaterial were studied, which are 0.5% and 1%. In all cases, the tilt angle will be zero so the PV module becomes in a horizontal position.

Table 3: Thermo-physical properties of PCM (RT25HC) [Charles Divyateja et al., 2021] and Ag [Büyük Öğüt, 2009].

properties	PCM (RT25HC)		Ag
ρ (kg/m^3)	Solid	785	10500
	Liquid	749	
C_p (J/kg. K)	Solid	1800	235
	Liquid	2400	
Thermal Conductivity (W/m. K)	Solid	0.19	429
	Liquid	0.18	
Melting Temperature (°C)	26.6		
L (J/kg)	232000		
Dynamic Viscosity (kg/m. s)	0.001798		

4.2 Numerical model

The heat transfer diffusion equation has been utilized for the PV, Al box and PCM, which takes the form below [Kant et al., 2016b]:

$$\rho C_p \frac{\partial T}{\partial t} + \nabla.(-k\nabla T) + \rho C_p \vec{u}\,.\nabla T = 0 \qquad (1)$$

ρ, C_p and k represent the density, specific heat and thermal conductivity, respectively. $\vec{u}$ is velocity field (m/s). T and t denote the temperature and time respectively. This equation consists of three terms. The First one represents the rate of temperature's change in the solid or fluid region, also known as the unsteady term. The second term is the heat flux due to conduction. The last one represents convection energy transfer [Ansys Fluent Theory Guide]. In the solid parts of the system, the convection energy transfer term and velocity field equal zero, and so equation (1) becomes:

$$\rho \mathrm{C}_p \frac{\partial T}{\partial t} = 0 \qquad (2)$$

The density and TC of the PCM depend on the PCM's temperature. They were modeled as [Kant et al., 2016b]:

$$\rho_{PCM}(T) = \rho_{solid} + \left(\rho_{liquid} - \rho_{solid}\right) B(T) \qquad (3)$$

$$k_{PCM}(T) = k_{solid} + \left(k_{liquid} - k_{solid}\right) B(T) \qquad (4)$$

Function B (T) given as:

$$B(T) = \begin{cases} 0, & T < T_m - \Delta T \\ \dfrac{T - T_m + \Delta T}{2\,\Delta T}, & T_m - \Delta T \le T \le T_m + \Delta T \\ 1, & T > T_m + \Delta T \end{cases} \qquad (5)$$

When $T < T_m - \Delta T$, PCM will be in the solid state, B(T) equals zero, so $\rho_{PCM}(T)$ and $k_{PCM}(T)$ equal ρ_{solid} and k_{solid} respectively. When $T > T_m + \Delta T$, PCM will be in the liquid state, B(T) equals one, so $\rho_{PCM}(T)$ and $k_{PCM}(T)$ equal ρ_{liquid} and k_{liquid} respectively. In interval $[T_m - \Delta T, T_m + \Delta T]$, PCM will be in the transition zone, B(T) changes linearly and so both $\rho_{PCM}(T)$ and $k_{PCM}(T)$ will be changed.

The specific heat of PCM was modeled as [Kant et al., 2016b]:

$$\mathrm{C}_{p\,PCM}(T) = \mathrm{C}_{p\,solid} + \left(\mathrm{C}_{p\,liquid} - \mathrm{C}_{p\,solid}\right) B(T) + L\,D(T) \qquad (6)$$

Function D(T) given as:

$$D(T) = e^{\left(\frac{-(T-T_m)^2}{\Delta T^2} / \sqrt{\pi\,.\,\Delta T^2}\right)} \qquad (7)$$

D is a function that depends on temperature, thus, the PCM's specific heat changes when the temperature of PCM changes. D is a function that always equals zero, except in the transition region. So, $C_{p_{PCM}}(T)$ equal $C_{p_{solid}}$ and $C_{p_{liquid}}$ are in solid phase and liquid phase respectively. In transition region, $C_{p_{PCM}}(T)$ is changeable according to the equation (5).

The viscosity of PCM also depends on the temperature which was modeled as [Groulx et al., 2020; Charles Divyateja et al., 2021]:

$$\mu(T) = \mu_l \left(1 + A(T)\right) \tag{8}$$

And A(T) given as:

$$A(T) = \frac{c_m (1 - B(T))^2}{B(T)^3 + \varepsilon} \tag{9}$$

c_m is a constant value which ranges between 10^4 and 10^7 [Kant et al., 2016b]. In our study, the value of c_m is 10^6 because the PCM viscosity is high in the solid state. ε equals 10^{-3}, which is an extremely small number to avoid division by zero when B(T) equals zero.

After adding Ag nanoparticles or Ag nanowires to PCM, the PCM's thermo-physical properties will be changed. The density and specific heat for the NPCM were got from [Vajjha et al., 2010; Zarma et al., 2017; Sushobhan and Kar, 2017; Khanjari et al., 2016]

$$\rho_{NPCM} = \varphi\rho_{np} + (1 - \varphi)\rho_{pcm} \tag{10}$$

$$C_{p_{NPCM}} = \frac{\varphi(\rho C_P)_{np} + (1 - \varphi)(\rho C_P)_{pcm}}{\rho_{NPCM}} \tag{11}$$

φ is the volume fraction of nanoparticles or nanowires.

The latent heat for NPCM given as [Zarma et al., 2017; Sushobhan and Kar, 2017]:

$$L_{NPCM} = \frac{(1 - \varphi)\,(\rho L)_{pcm}}{\rho_{NPCM}} \quad (12)$$

Batchelor's model is used to express the viscosity for NPCM [Batchelor, 1977; Qiu et al., 2020; Zhu et al., 2018]:

$$\mu_{NPCM} = (1 + 2.5\varphi + 6.2\varphi^2)\,\mu_{PCM} \quad (13)$$

Thermal conductivity for NPCM is expressed by Hamilton model. Because this model takes into consideration the shape of nanomaterials [Hamilton & Crosser, 1962; Fang et al., 2014];

$$k_{NPCM} = \frac{k_{np} + (n-1)k_{PCM} - (n-1)\varphi(k_{PCM} - k_{np})}{k_{np} + (n-1)k_{PCM} + \varphi(k_{PCM} - k_{np})}\,k_{PCM} \quad (14)$$

Where $n = 3/\Psi$, and Ψ is sphericity. n equals 3 for spherical nanomaterial (nanoparticle). The diameter of the nanoparticles was considered 50 nm. For nanowire, n equals 17.12, Ψ was calculated according the equation $\Psi = \frac{\pi^{\frac{1}{3}}(6V)^{\frac{2}{3}}}{A}$. Where V and A are the volume of nanowire and surface area of nanowire respectively. In this study, the diameter of the nanowires was considered 60 nm and the length 25 μm as in [Gu et al., 2013].

When hybrid nanomaterials were used to improve PCM, we obtained new properties for the resulting material. The thermophysical properties of hybrid nanoPCM (HNPCM) can be presented through the following mathematical equations [Ghadikolaei et al., 2017; Faraji et al., 2021]:

$$\rho_{HNPCM} = (1 - \varphi_2)[(1 - \varphi_1)\,\rho_{PCM} + \varphi_1\,\rho_{s1}] + \varphi_2\,\rho_{s2} \quad (15)$$

$$C_{p\,HNPCM} = \frac{(1 - \varphi_2)\big[(1 - \varphi_1)(\rho\,C_p)_{PCM} + \varphi_1(\rho\,C_p)_{s1}\big] + \varphi_2(\rho\,C_p)_{s2}}{(\rho)_{HNPCM}} \quad (16)$$

$$\mu_{HNPCM} = \frac{\mu_{PCM}}{(1 - \varphi_1)^{2.5}(1 - \varphi_2)^{2.5}} \quad (17)$$

$$L_{HNPCM} = \frac{(\rho L)_{PCM}(1 - \varphi_1)(1 - \varphi_2)}{(\rho)_{HNPCM}} \quad (18)$$

$$k_{HNPCM} = \frac{k_{s2} + (n_2 - 1)k_{bPCM} - (n_2 - 1)\varphi_2(k_{bPCM} - k_{s2})}{k_{s2} + (n_2 - 1)k_{bPCM} + \varphi_2(k_{bPCM} - k_{s2})} k_{bPCM} \quad (19)$$

Where

$$k_{bPCM} = \frac{k_{s1} + (n_1 - 1)k_{PCM} - (n_1 - 1)\varphi_1(k_{PCM} - k_{s1})}{k_{s1} + (n_1 - 1)k_{PCM} + \varphi_1(k_{PCM} - k_{s1})} k_{PCM} \quad (20)$$

φ_1 and φ_2 are the volume fraction of nanoparticles and nanowires respectively.

4.3 Numerical simulation

There are two methods that can be used to simulate the phase change process. These methods are the effective heat capacity method and the enthalpy porosity (EP) method [García-Fuente et al., 2022; Reichl et al., 2022]. For more information about these two methods, you can refer to Reichl's article [Reichl et al., 2022].

In this work, EP method is used by activating the solidification and melting model in Ansys Fluent. In this technique, the melt interface is not tracked explicitly. Instead, a quantity called the liquid fraction, which indicates the fraction of the cell volume that is in liquid form, is associated with each cell in the domain. The liquid fraction is computed at each iteration, based on an enthalpy balance. The mushy zone is a region in which the liquid fraction lies between 0 and 1. The mushy zone is modeled as a "pseudo" porous medium in which the porosity decreases from 1 to 0 as the material solidifies. When the material has fully solidified in a cell, the porosity becomes zero and hence the velocities also drop to zero [Ansys Fluent Theory Guide].

Case I:

Solidworks software was used to create 3D geometry for prevailing PV panel that consist of five layers. The 3D geometry for prevailing PV panel was designed with dimensions 160*100*4.4 mm, 4.4 mm is the PV's thickness, which is the sum of the five layers' thickness that make up the PV mentioned in table 2. Then, the mesh was created on Ansys fluent software after importing the geometry (the mesh details are mentioned in appendix A). After that, the pressure-based solver and transient state options were selected. Next, the gravity was added. In physics models, we specified the energy equation to solve heat transfer in the PV's five solid layers. The layers' thermo-physical properties, which are shown in table 2, are fixed. Then, initial and boundary conditions were defined. In solution methods, SIMPLE scheme was selected for Pressure–Velocity Coupling. Also, PRESTO! scheme was chosen for the pressure equation. Second Order Upwind was specified for momentum and energy equation. For the energy equation, convergence criteria was set at 10^{-6} but it was 10^{-4} for the rest of the equation. Time step size was 1 s and maximum iterations per time step was 20.

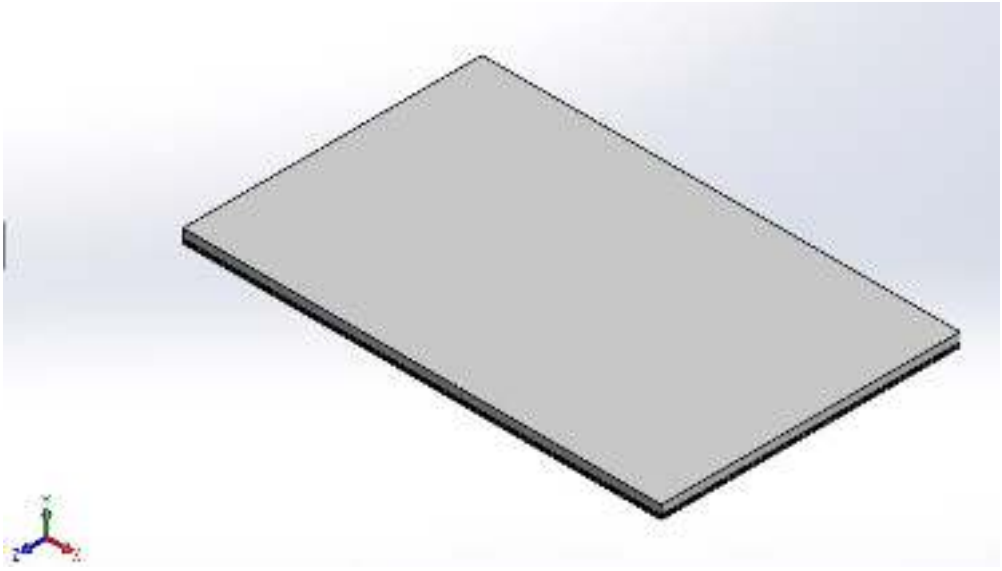

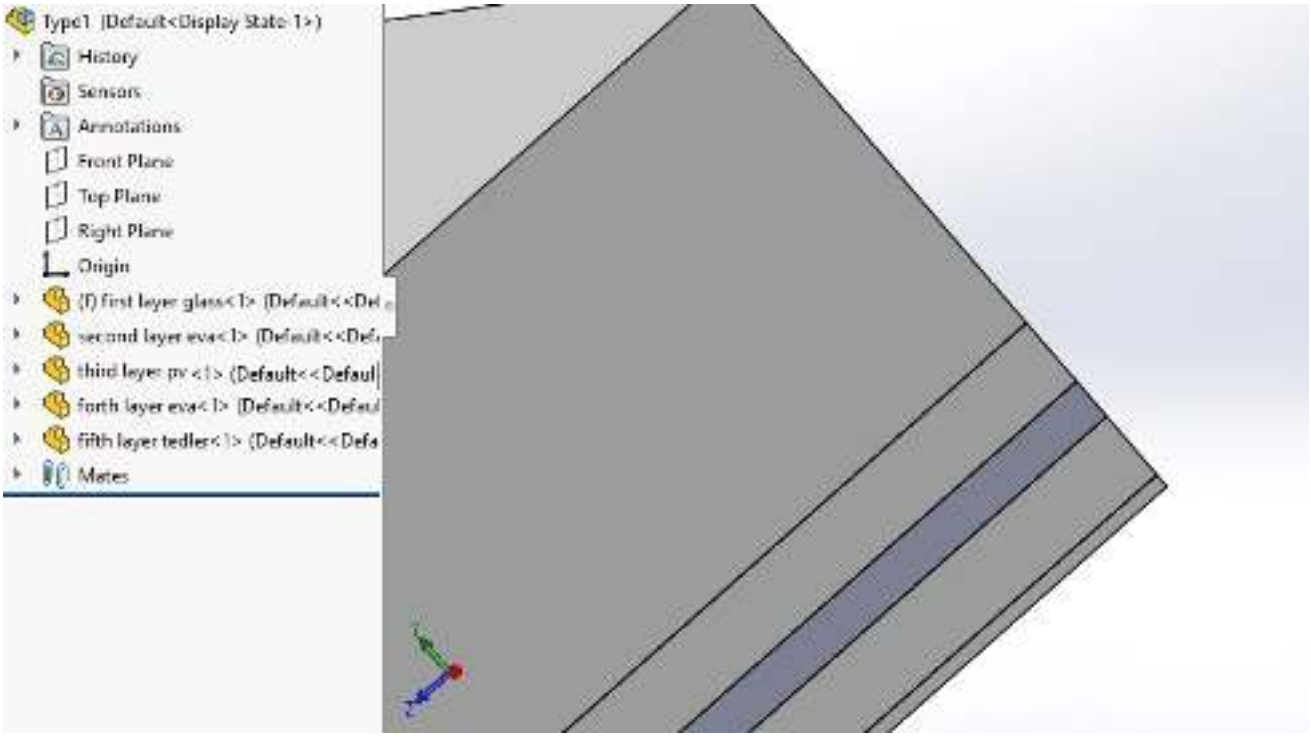

Figure 7: 3D geometry of PV on Solidworks.

Cases from 2 to 5:

Solidworks software was used to create 3D geometry that shown in figure 6, which was with dimensions 160*100*28.4 mm, 28.4 mm is the thickness of the PV-PCM, which is the sum of all layers' thickness that make up the PV-PCM that was mentioned in table 2. Figure 8 represents the 3D geometry of the PV-PCM made on Solidworks. All steps and procedures were done identically as in case 1, but in physics models, both the "viscous - laminar flow" and "solidification and melting", as well as energy equation were all specified. The PCM's thermo-physical properties were defined using a user-defined function (UDF) (the UDF details are mentioned in appendix B), then; they were compiled to the Ansys fluent solver.

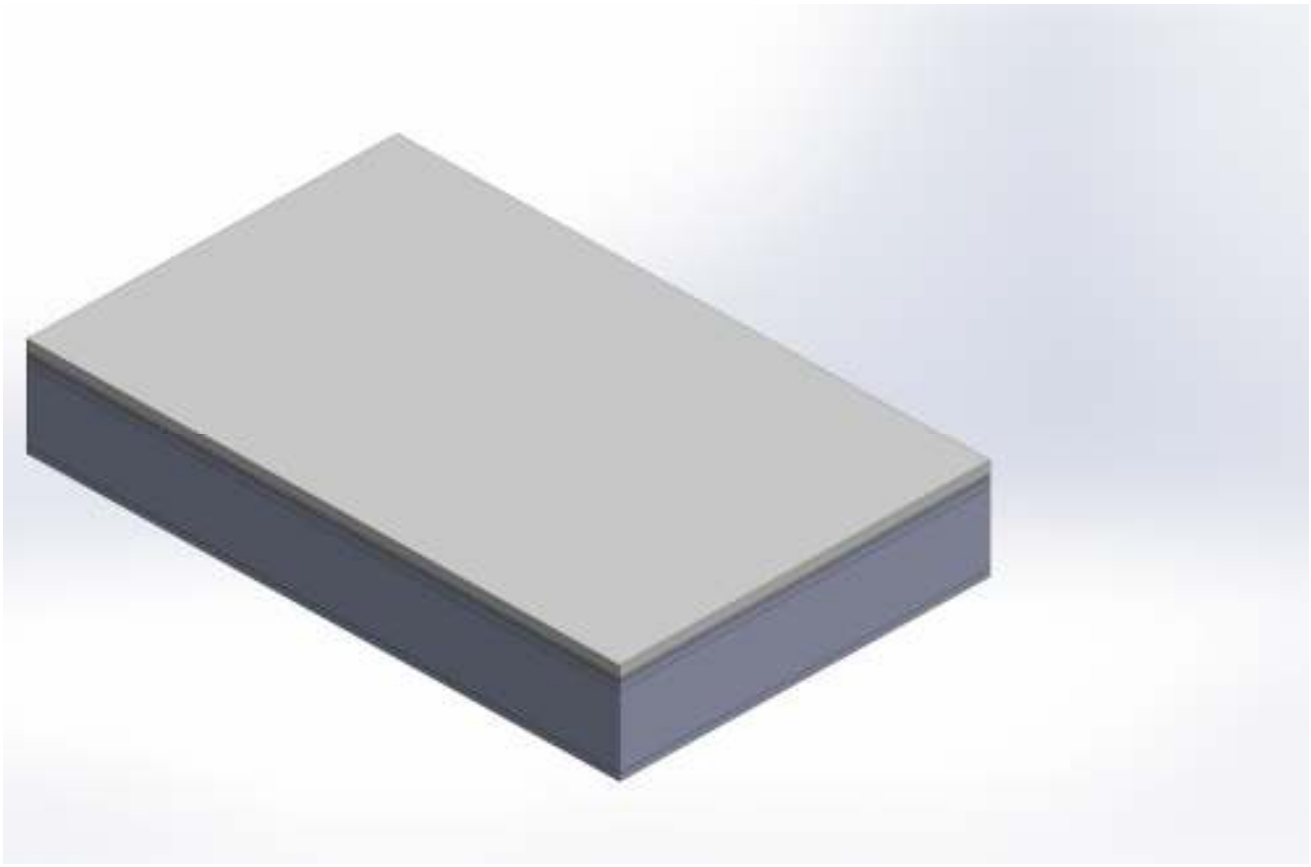

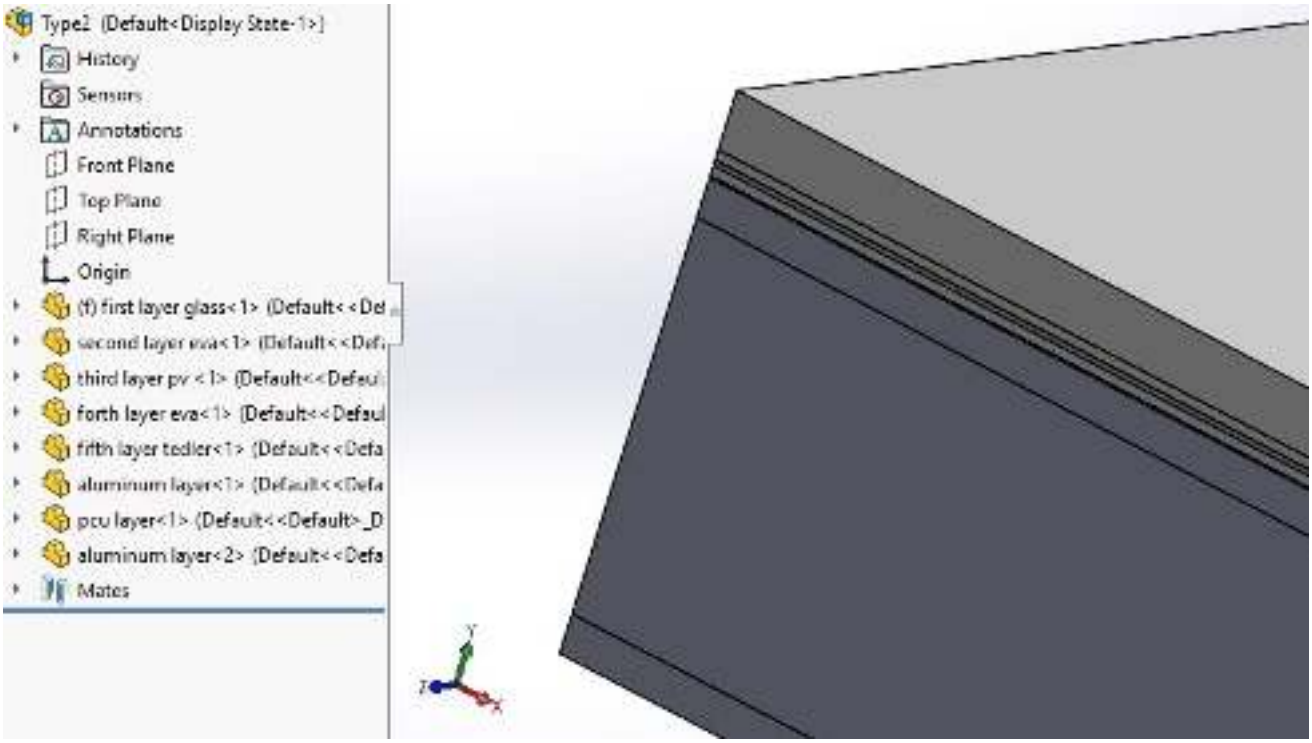

Figure 8: 3D geometry of the PV-PCM on Solidworks.

In all cases, a profile was created that includes the temperature of PV module versus time during 120 minutes (2 hours). Then equation (21) was used to compute the PV's efficiency during that period.

$$\eta_{PV} = \eta_c \left(1 - \beta_o \left(T_{PV} - 298.15\right)\right) \quad (21)$$

Where β_o is constant equal $0.0045\ ℃^{-1}$ for crystalline PV. η_c is the PV efficiency at the reference temperature. η_c = 15% at 298.15 K [Lee & Tay, 2012].

Simulation steps are explained in figure 9. In our simulation, the following assumptions and limitations were taken into account in all cases:

- All materials have constant thermo-physical characteristics except PCM.
- The PCM's thermo-physical properties depend on the PCM's temperature.
- Solar radiation is constant and equal in all parts of the solar panel's upper surface (solar radiation = 1000 W/m^2).
- PV module is in a horizontal position; tilt angle is zero.
- The impact of dust was neglected.
- The system's initial temperature equals the ambient temperature (T_{amb} = 20 °C).
- The sidewalls of all layers were insulated.
- Emissivity of the System's top and bottom surfaces were 0.91 and 0.85 respectively [Kant et al., 2016b].
- Reflectivity, absorptivity and transitivity of glass were respectively equal 0.04, 0.04 and 0.92 [Wodołażski et al., 2021; Lamaamar et al., 2022].
- Transitivity of EVA layer, silicon layer and tedlar were respectively equal 0.9, 0.02 and 0 [Wodołażski et al., 2021].
- The reflected solar radiation of the inner layers' surface (EVA, silicone and tedlar) was neglected.
- Heat transfer coefficients of the system's top and bottom surfaces were 10 $W/m^2\ K$ and 5 $W/m^2\ K$ respectively [Charles Divyateja et al., 2021].
- Transient state.

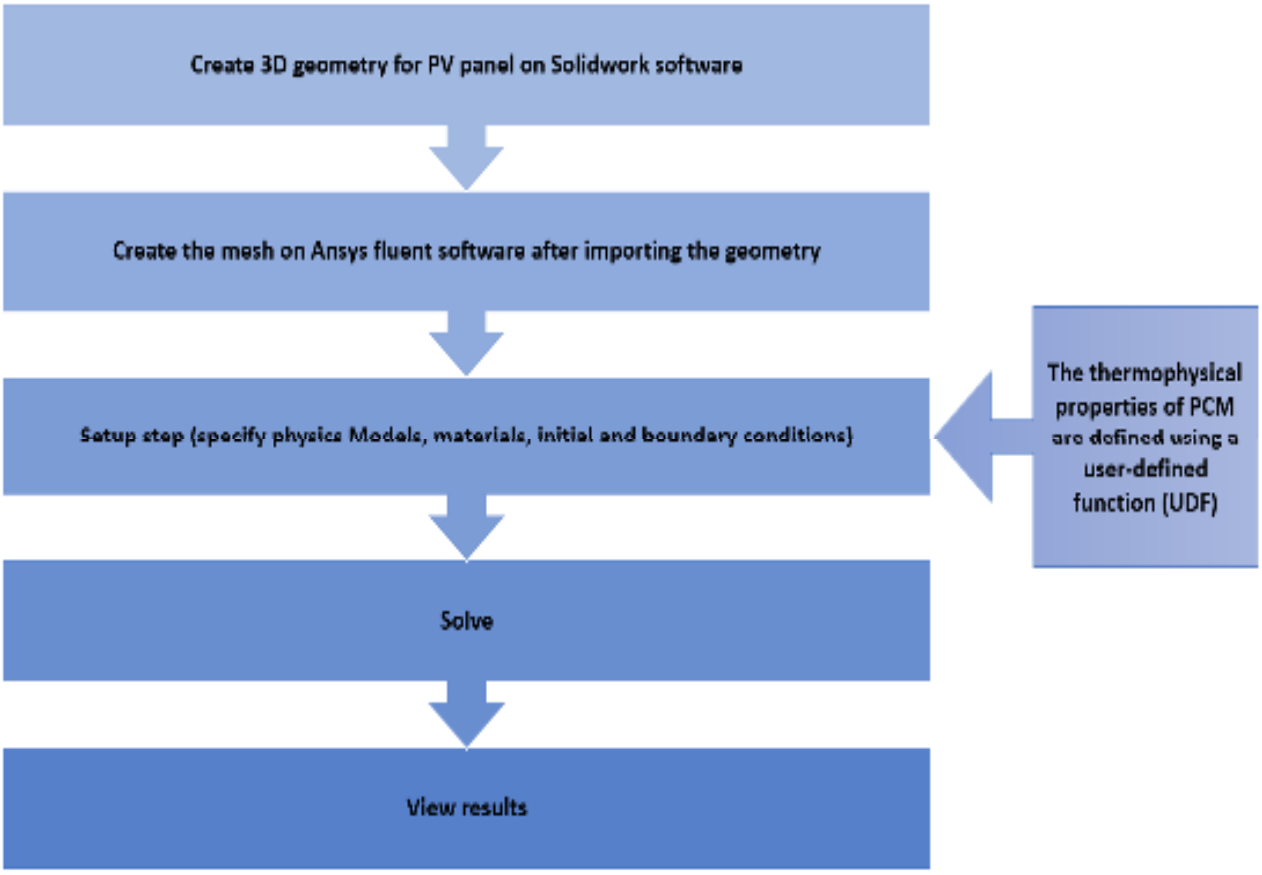

Figure 9: Simulation steps.

CHAPTER 5: Results and discussion

A study was done to analyze the heat transfer in the PV, PV with PCM, and PV with PCM enhanced by nanomaterials (nanoparticles, nanowires and nanohybrid), this was done when the PV was exposed to a constant solar radiation equals 1000 W/m^2. Also, the study clarified the change in the temperature of the PV during two hours and the effect on its efficiency.

This chapter includes two parts. The first one explains the temperature's effect on the thermophysical properties of the PCM and the PCM that improved by using nanomaterials, and it compares between them. In the second part, we present and discuss the findings obtained after conducting the simulation within assumptions by “Ansys fluent” software. These assumptions were mentioned in the previous chapter.

5.1 The impact of temperature on thermophysical properties.

In the previous chapter, it was pointed that the thermophysical properties of PCM, NPCM and HNPCM depend on temperature. By analyzing and comparing equations 3-20, it was noticed that adding nanomaterials to PCM increased its TC.

Figure 10 represents the relation between the TC and the temperature of PCM, NPCM and HNPCM, which shows that the increase in the nanomaterials' volume fraction leads to an increasing in the TC. The PCM enhanced by nanowires at $\varphi = 1\%$ had the highest thermal conductivity, followed by the PCM enhanced using nanohybrid at $\varphi = 1\%$. However, the PCM without nanomaterials had the lowest thermal conductivity.

Otherwise, the addition of nanomaterials to the PCM led to a decrease in both specific heat and latent heat. The latent heat and the specific heat of the PCM decrease when the volume fraction of the nanomaterials increases. Figure 11 represents the comparison among the TC and the latent heat of PCM, NPCM and HNPCM. The largest decline in the specific heat of the PCM occurred when PCM improved by using nanoparticles or nanowires at $\varphi = 1\%$. By conducting a comparison between the latent heat of the PCM, NPCM and HNPCM, the lowest latent heat was for the NPCM at $\varphi = 1\%$.

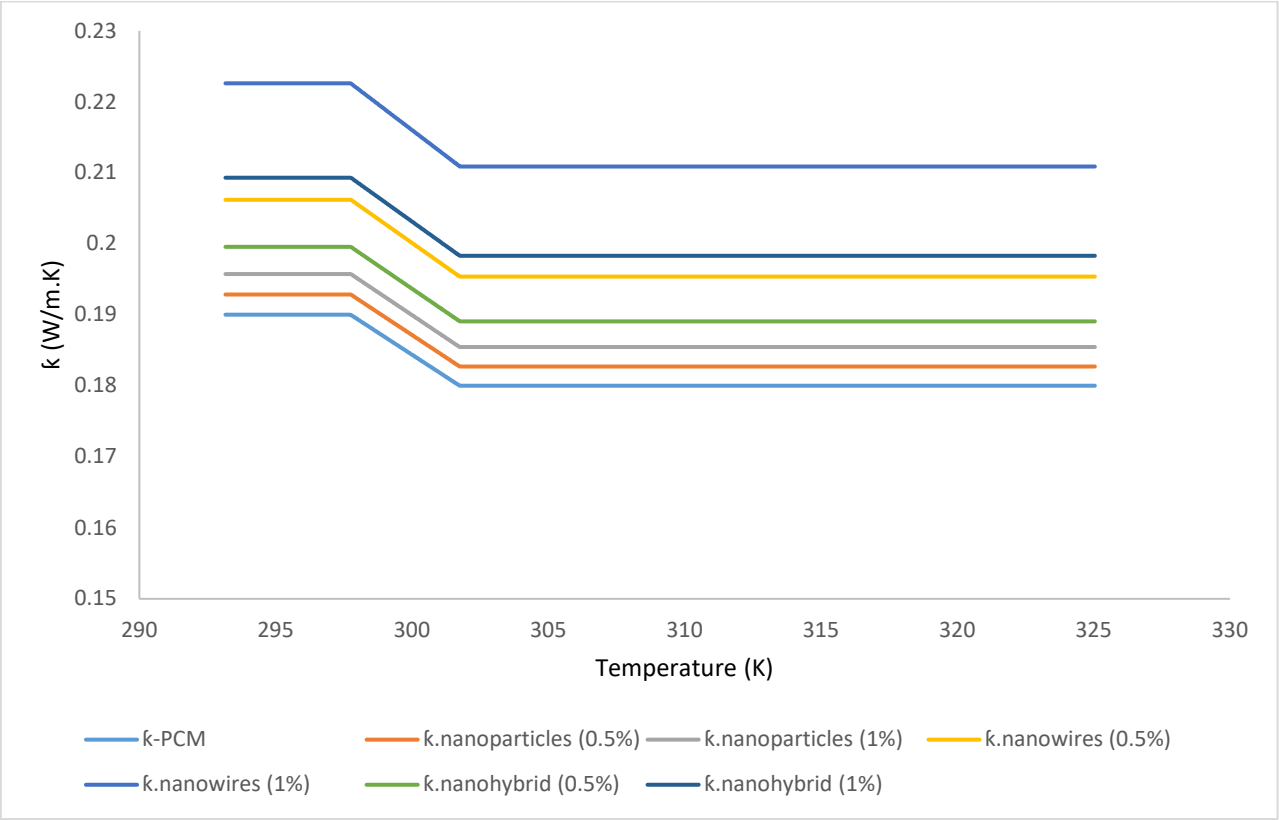

Figure 10: Comparison of TC between PCM, NPCM and HNPCM.

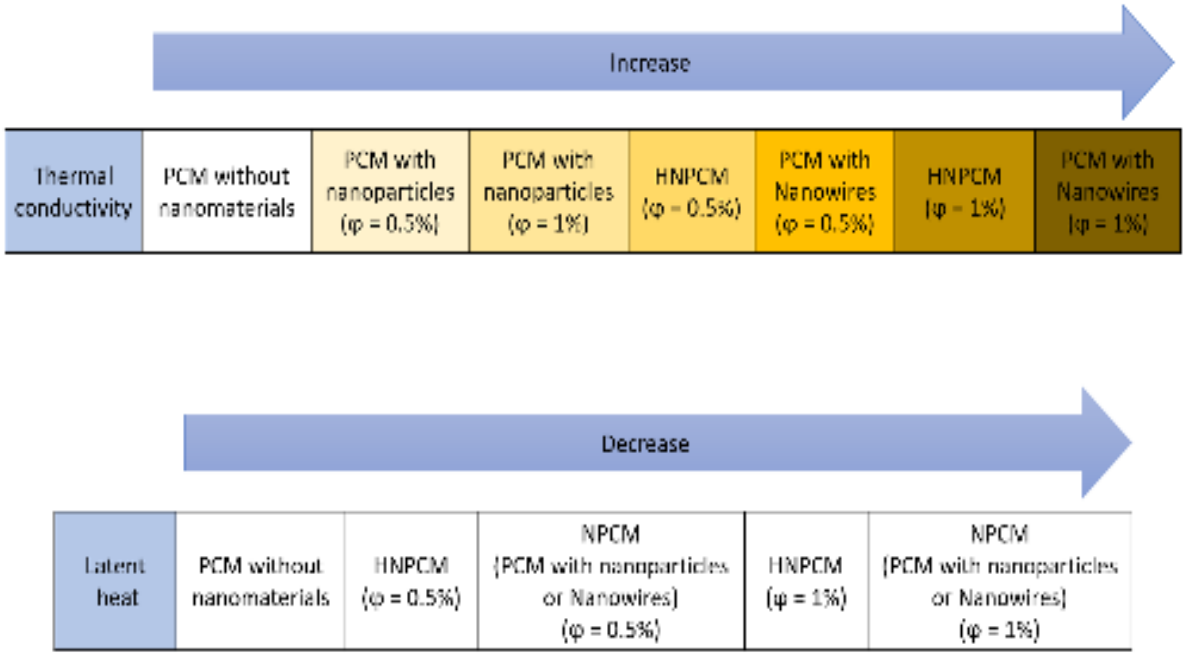

Figure 11: The comparison between the TC and the latent heat of PCM, NPCM and HNPCM.

5.2. PV temperature.

Through simulation in Ansys fluent, a profile was created which includes the change in the PV's temperature versus the time during two hours. Then, the average temperature and efficiency of PV were calculated for 2h. After that, the results for each case were compared with case 1.

5.2.1 Case I: PV without PCM.

In this case, we analyzed the PV's thermal performance without PCM and in a horizontal position. The PV contains five solid layers, and the heat transfers through these layers by conduction.

Figure 12 shows the change in PV's temperature within two hours. The initial temperature was 20 °C (293.15 K). During the first seven minutes, the temperature of PV raised rapidly. Then, in the next 19 min, the temperature increased slightly. After about 26 min, the PV temperature reached 325.4 K. Then, the temperature remained almost constant until the end of the two hours. The temperature equals 325.473 K at t = 2 h. The PV's average temperature during two hours was 324.2767 K. According to equation (21), this increase in the PV's temperature negatively affect its efficiency.

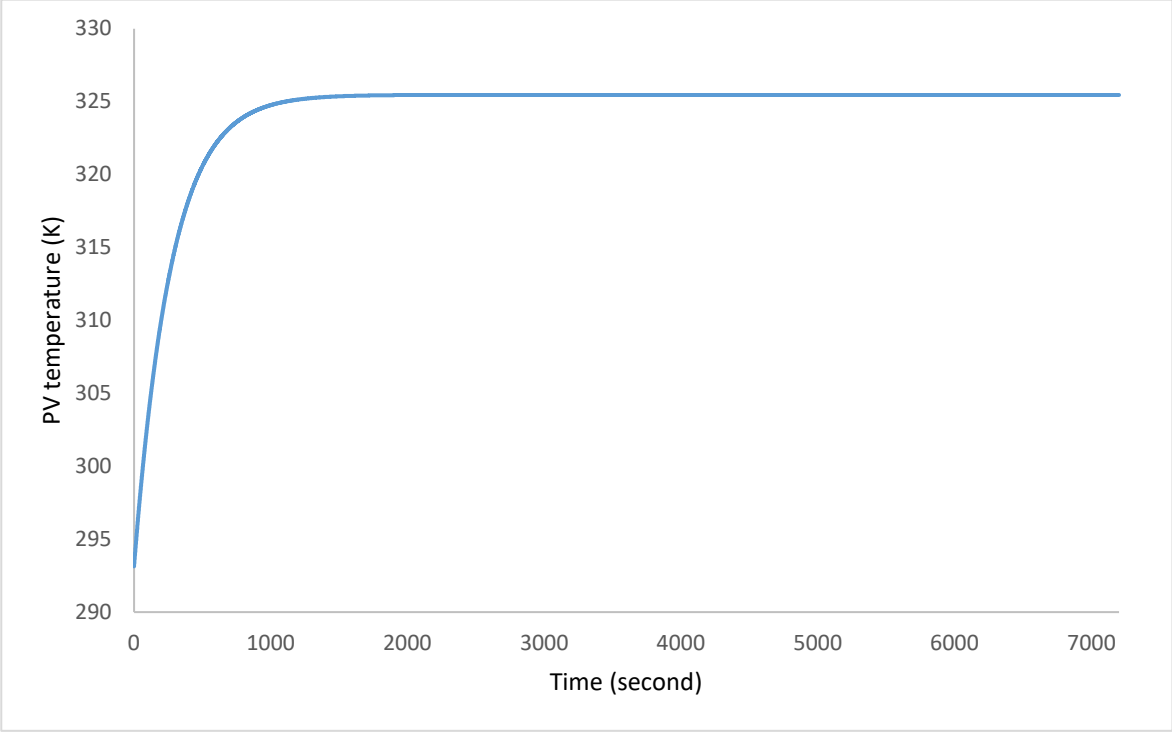

Figure 12: The temperature of PV during two hours.

5.2.2 Case II: PV with PCM.

The PCM was added to the PV to reduce PV's temperature. Figure (13) displays the PV−PCM system's temperature. The heat transfers via conduction through the PV layers and aluminum layer to PCM. When the PCM's temperature reaches $T_m - \Delta T$, the melting process begins. Which means storing the energy in PCM as latent heat form (PCM charging).

Figure 13 shows the temperature of PV−PCM within two hours. The system's initial temperature was 20°C (293.15 K). Almost during the first six minutes, the temperature was rising rapidly. Then, it became very slight, this period is the period which the PCM was melting during it. After that, the temperature returned to rise rapidly to 325 K. The temperature was 325.0409 K at t = 2 h. The average temperature during two hours was 314.0972 K., comparing this with case 1, it is noticed that there is a decline in the average temperature by approximately 10.2 degrees within 2 h. In addition, the efficiency of PV increased about 5.2%.

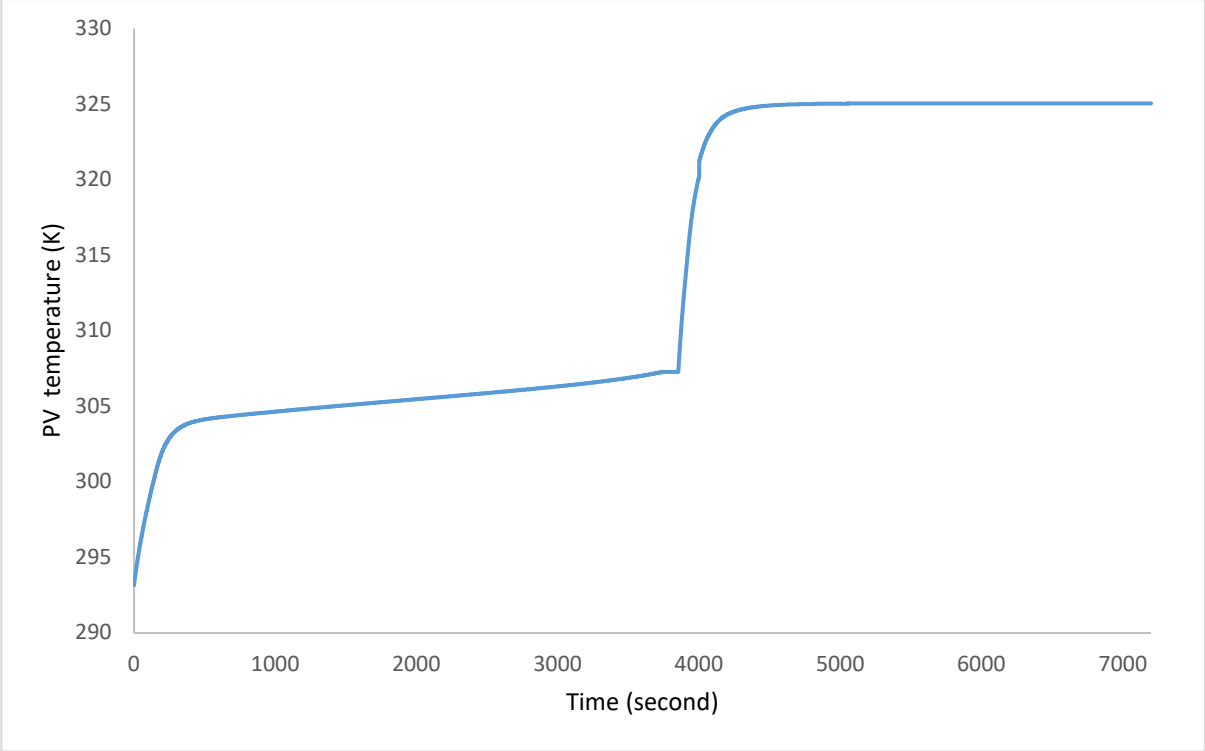

i

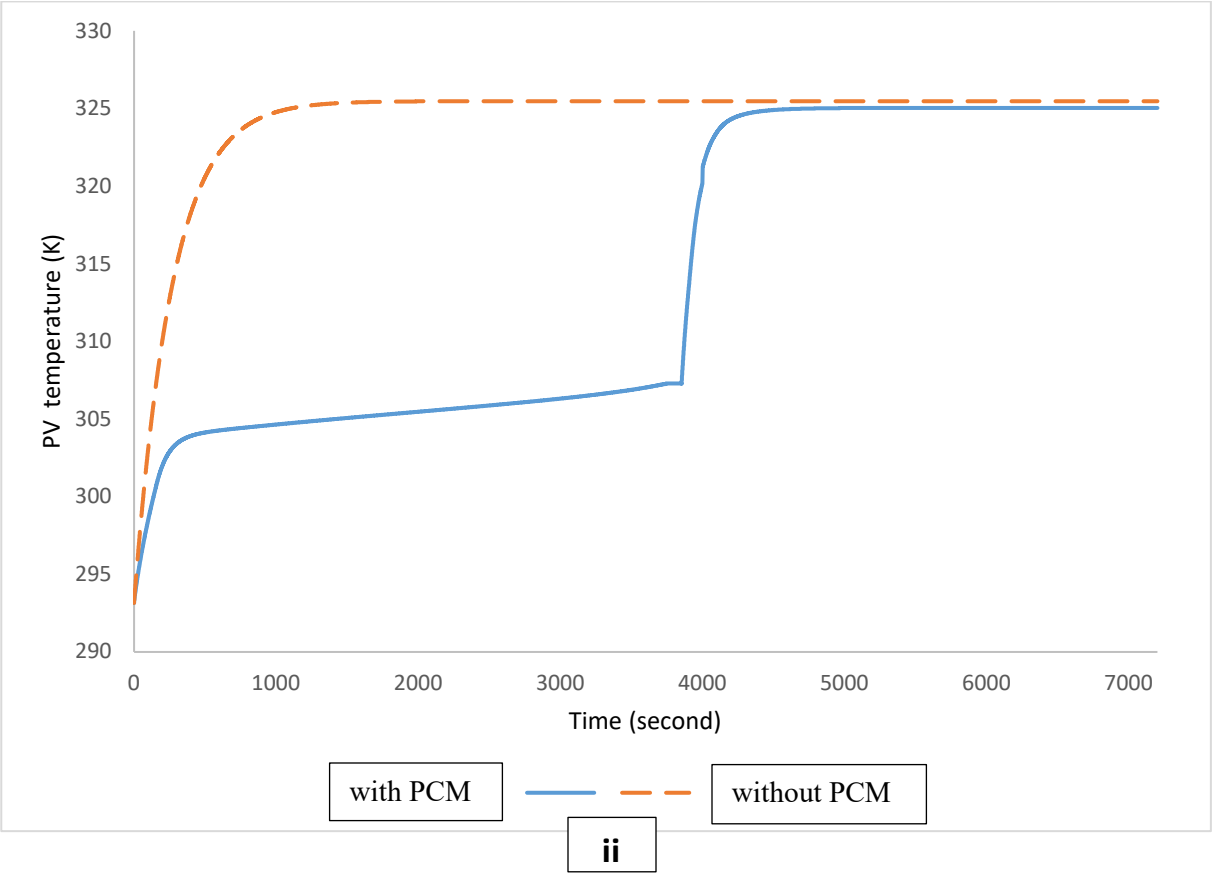

Figure 13: (i) The temperature of PV−PCM within two hours, (ii) The temperature's comparison between PV with and without PCM.

5.2.3 Case III: PV with PCM enhanced by nanoparticles.

The poor TC of PCM reduces its ability to decline the PV's temperature. The PCM was enhanced by nanoparticles to increase its TC. In this case, the impact of two volume fractions of nanoparticles (0.5% and 1%) were studied. Adding nanoparticles to PCM resulted in a rise in its TC and a reduction in its latent heat.

Figures 14 and 15 show the temperature of PV−NPCM. At first, the temperature was rising rapidly. Then, the rising became slight. After a while, the temperature returned to rise rapidly, and then it became almost constant. At t = 2 h, the PV's temperature was 323.041 K when $\varphi = 0.5\%$ and 319.639 K when $\varphi = 1\%$. The average temperature of PV during two hours was 312.8779 K and

311.389 K when φ equals 0.5% and 1% respectively. Comparing this case to case 1, the reduction in the average temperature was about 11.4 degrees and 12.9 degrees when $\varphi =$ 0.5% and 1% respectively. Moreover, the efficiency of PV increased about 5.8% and 6.6%. This is due to enhanced PCM by nanoparticles which leads to improve the heat transfer rate and the TC, and so increasing the PCM's ability to regulate the temperature of PV.

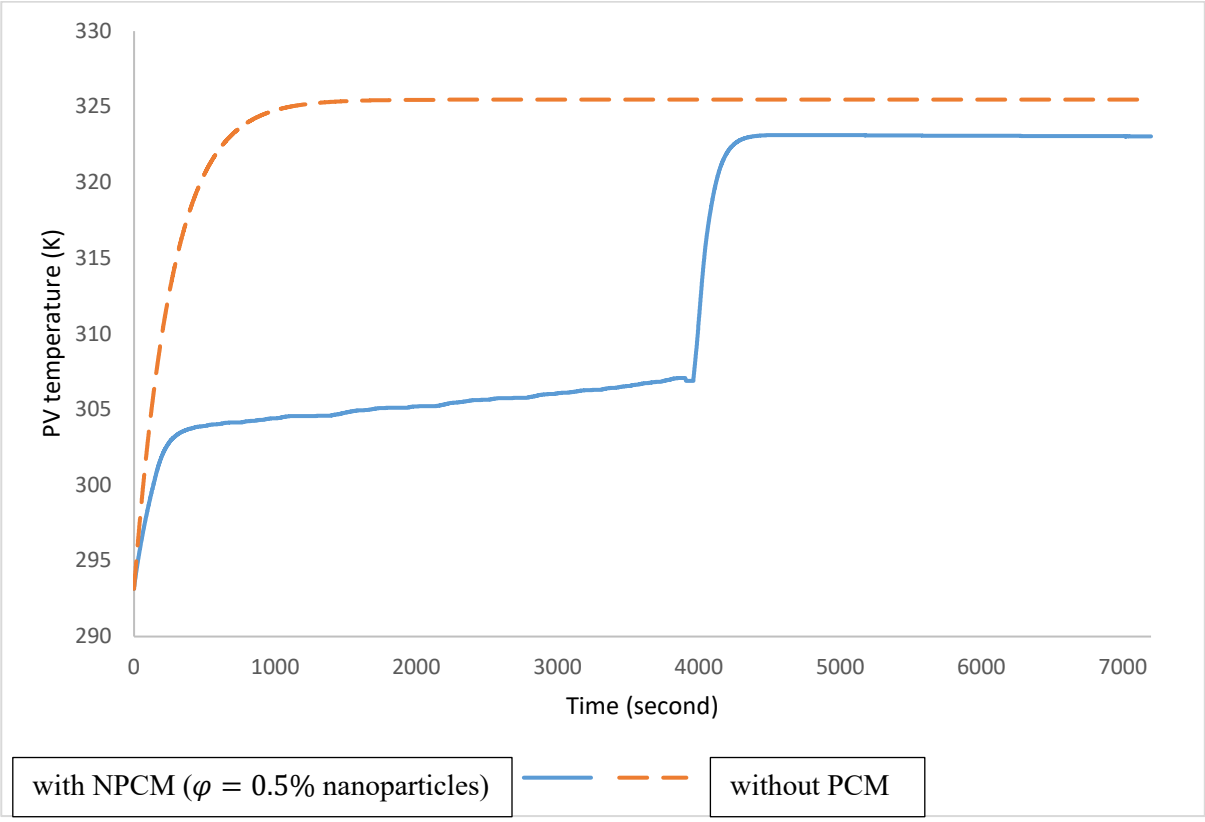

Figure 14: Comparison the temperature of PV−NPCM ($\varphi = 0.5\%$ nanoparticles) and PV without PCM.

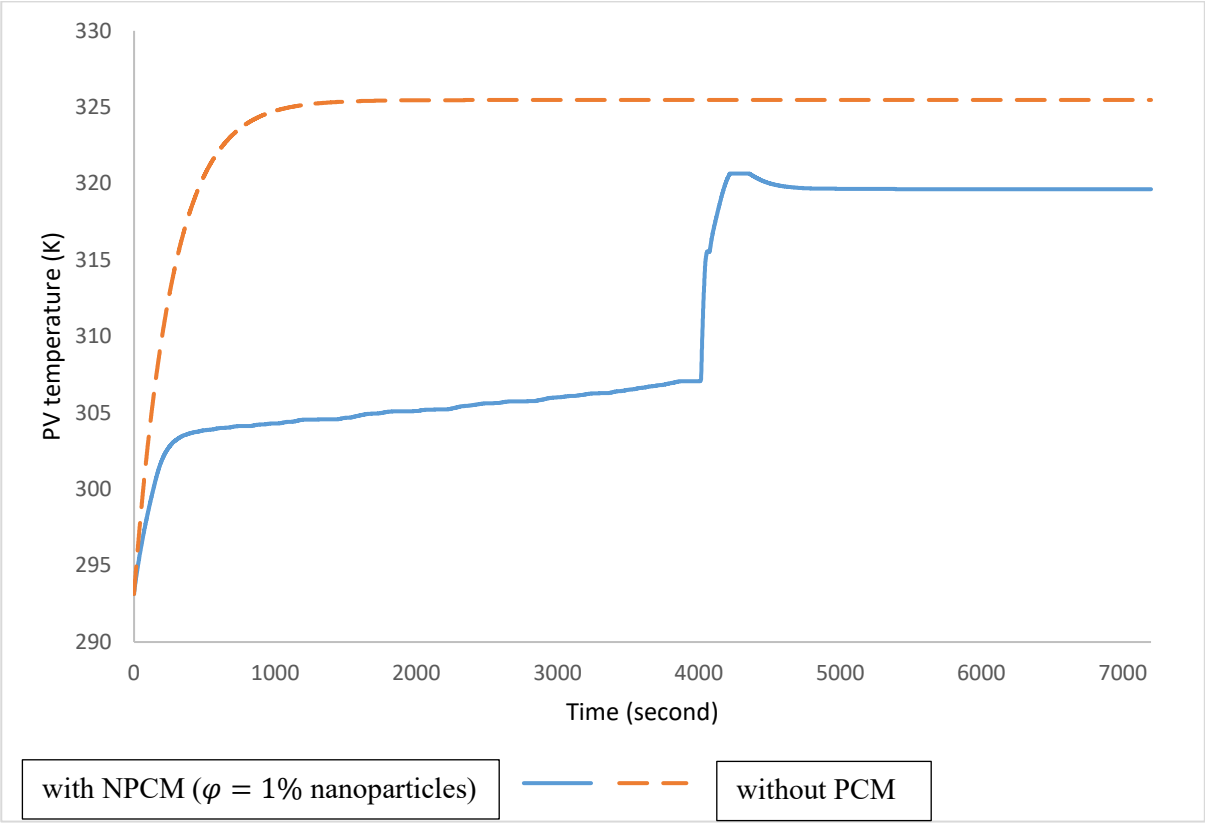

Figure 15: Comparison the temperature of PV−NPCM ($\varphi = 1\%$ nanoparticles) and PV without PCM.

5.2.4 Case IV: PV with PCM enhanced by nanowires.

In this case, the PCM was improved by using nanowires. The improved PCM using nanowires at $\varphi = 1\%$ has the best thermal conductivity and the least latent heat compared with PCM, PCM with nanoparticles and HNPCM. After conducting the simulation of PV-NPCM enhanced by nanowires, we obtained the following two figures. At t = 2 h, the PV temperature was 314.9707 K when $\varphi = 0.5\%$ and 321.7999 K when $\varphi = 1\%$. The average temperature of PV within 2 h was 309.3901 K and 312.7318 K when φ equal 0.5% and 1% respectively. By comparing the temperature of PV−NPCM ($\varphi = 0.5\%$ nanowires) and PV−NPCM ($\varphi = 1\%$ nanowires) with PV without PCM, we found out that the average temperature of PV declined by 14.9 degrees and 11.5 degrees when $\varphi = 0.5\%$ and 1% respectively. In addition, the efficiency of PV rose about 7.6% and 5.9%.

Although the TC of NPCM with 0.5% nanowires is less than the TC of NPCM with 1% nanowires, the first one gave better results in controlling and decreasing the temperature of PV, and this is due to the effect of increasing the volume fraction on the other thermophysical properties of PCM. The increasing in volume fraction creates a reduction in specific heat and latent heat of PCM.

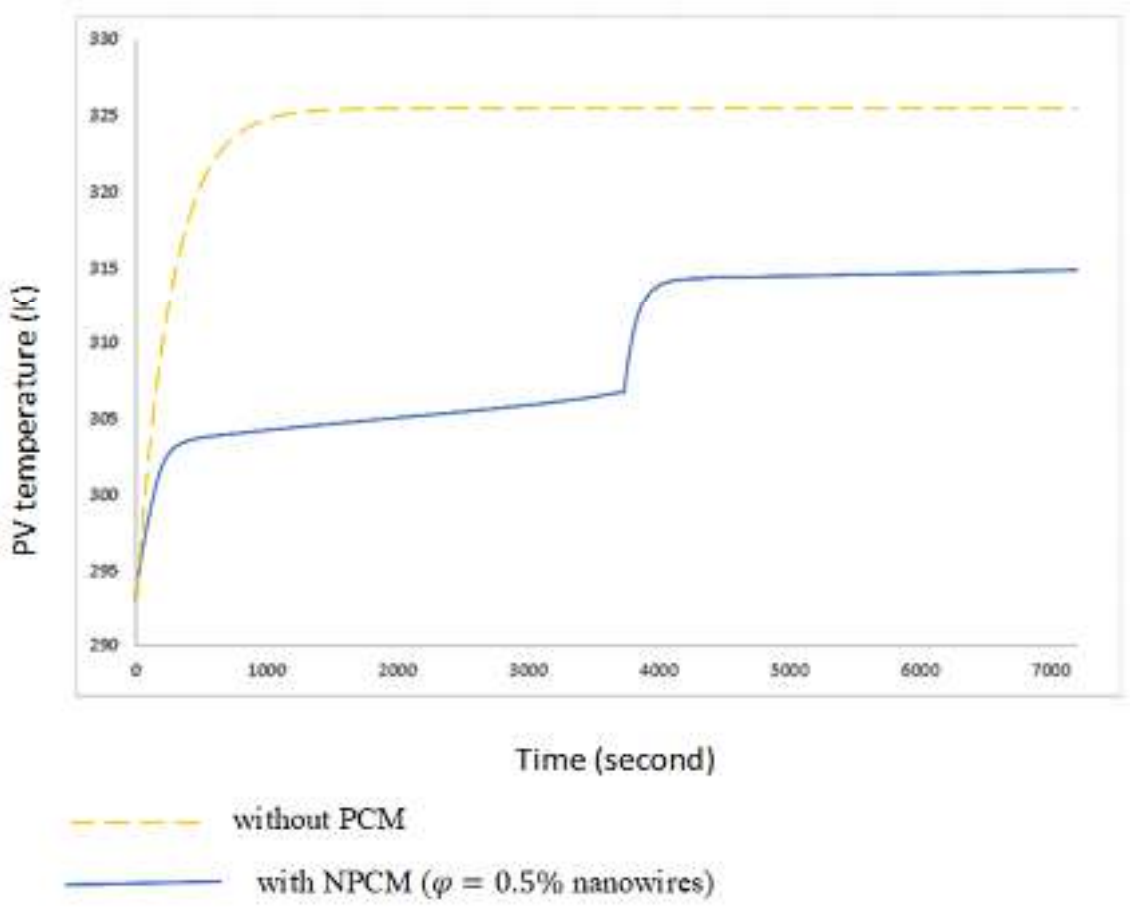

Figure 16: Comparison between the temperature of PV−NPCM ($\varphi = 0.5\%$ nanowires) and PV without PCM.

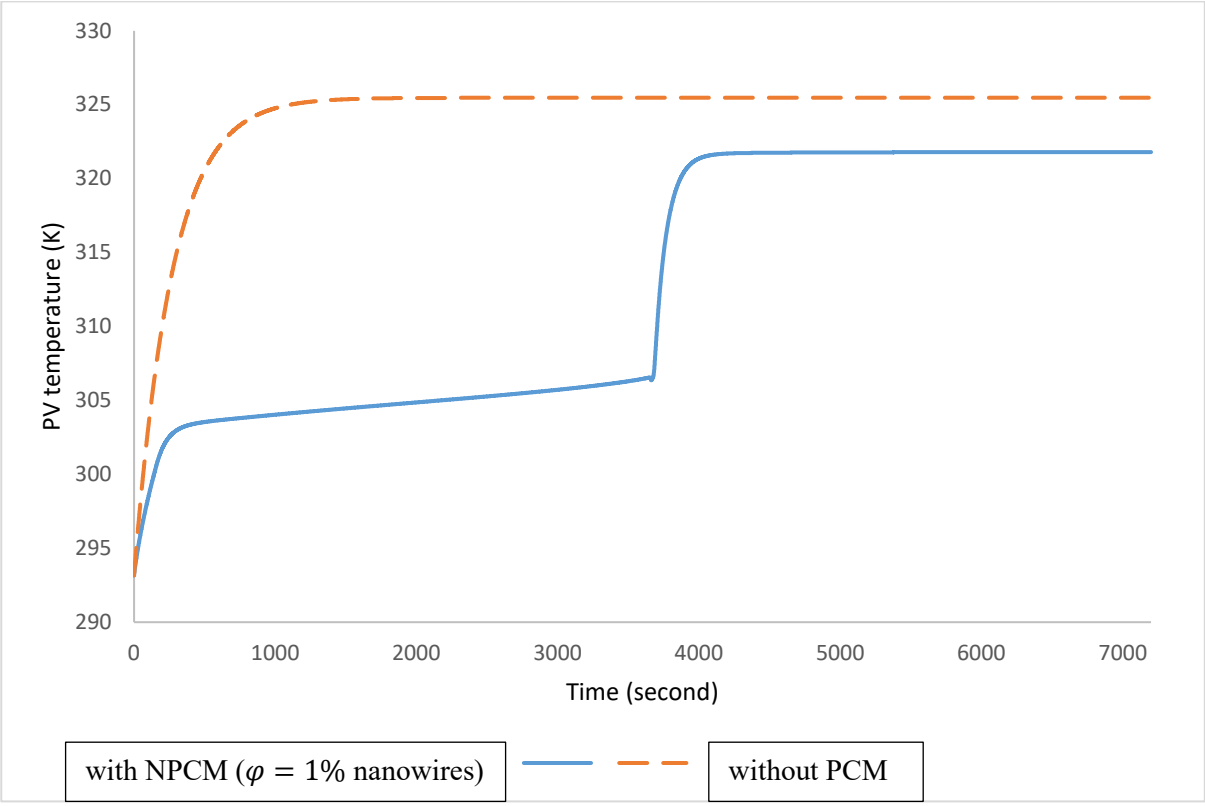

Figure 17: Comparison between the temperature of PV−NPCM ($\varphi = 1\%$ nanowires) and PV without PCM.

5.2.5 Case V: PV with PCM enhanced by nanohybrid.

In the last case, the PCM was enhanced by a hybrid of Ag nanoparticles and Ag nanowires with a percentage of (50%-50%). Figures 18 and 19 display the PV- HNPCM temperature with $\varphi = 0.5\%$ and 1%. The average temperature of PV during two hours was 312.1241 K and 312.1074 K when $\varphi = 0.5\%$ and 1% respectively. If we compared this case with the first case, the reduction in the average temperature was about 12.15 degrees and 12.17 degrees when $\varphi = 0.5\%$ and 1% respectively. Moreover, the efficiency of PV rose about 6.2%.

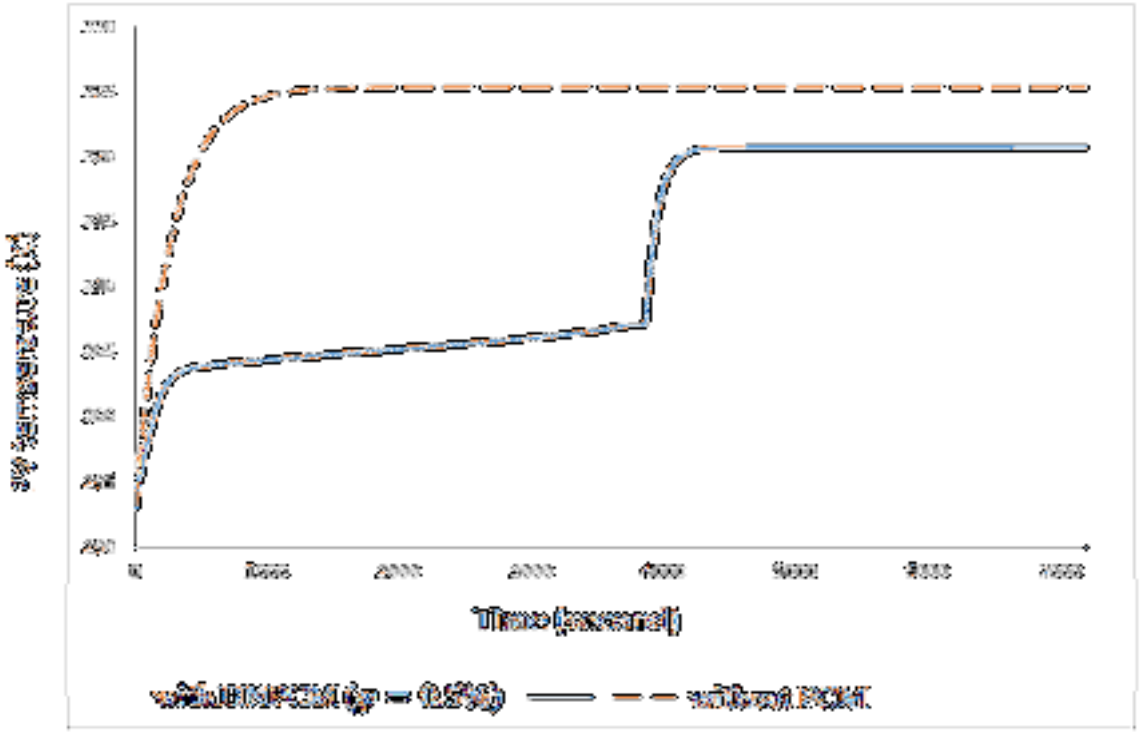

Figure 18: Comparison between the temperature of PV−HNPCM ($\varphi = 0.5\%$) and PV without PCM.

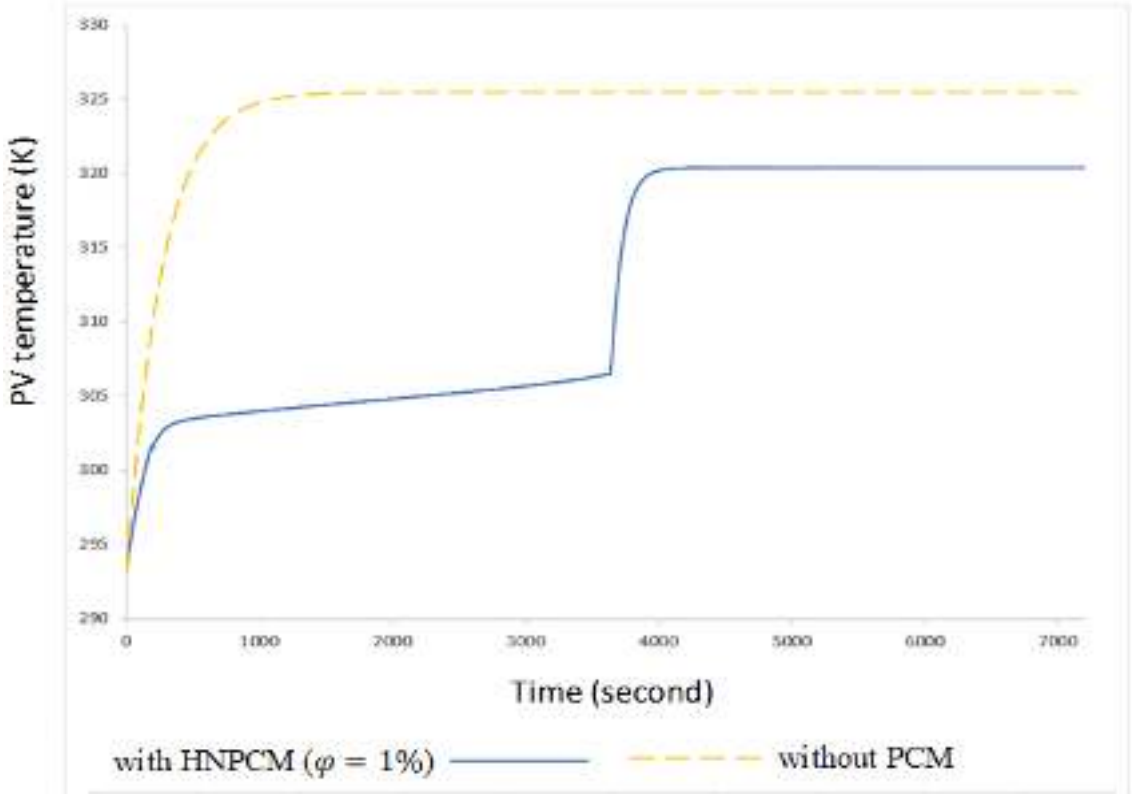

Figure 19: Comparison between the temperature of PV−HNPCM ($\varphi = 1\%$) and PV without PCM.

CHAPTER 6: Conclusion and Future Work

6.1 Conclusions

This thesis analyzes the possibility of enhancing the TC of PCM (which is paraffin) by adding different shapes of silver nanomaterials. Then, we examined the ability of these improved materials to regulate and reduce the PV's temperature to raise its efficiency. This thesis concentrates on the comparison of the ability of the enhanced PCM by different shapes of nanomaterials at two different volume fractions (1% and 0.5%) to minimize the PV's temperature.

The Solidworks software was used to build a 3D system of the PV and PV - PCM. Then, Ansys fluent software was used to simulate five cases; PV without PCM, PV with PCM, PV with PCM enhanced by silver nanoparticles, PV with PCM enhanced by silver nanowires and PV with PCM enhanced by nanohybrid.

After simulation and obtaining the results of the five cases, we compared the results, and we came up with the following conclusions:

- The nanomaterials' shape affects the PCM's thermos-physical properties. However, in all cases, increasing volume fraction of nanomaterial leads to a rise in the TC, and at the same time leads to a decline in the specific heat and latent heat.
- The PCM enhanced by nanowires at $\varphi = 1\%$ had the highest thermal conductivity, followed by the PCM enhanced using nanohybrid at $\varphi = 1\%$. And the largest decline in the latent heat of PCM occurred when PCM was improved using nanoparticles or nanowires at $\varphi = 1\%$. On the other hand, PCM enhanced by nanohybrid at $\varphi = 0.5\%$ has the highest latent heat.
- Using PCM enhanced by nanowire at $\varphi = 0.5\%$ gave the best results in decreasing the PV's temperature. The average temperature of PV lowered by 14.9 degrees. In addition, the efficiency of PV rose about 7.6%. Followed by using PCM enhanced by nanoparticles at $\varphi = 1\%$, the minimizing in the PV's average temperature was 12.9 degrees. Moreover, the efficiency of PV rose about 6.6%.

6.2 Future Work

- Expanding the study to include non-horizontal system.
- Studying the effects of other types of nanohybrid to improve PCM, which include 2D nanomaterials such as nanosheets.
- Expanding the study to include the solidification process.
- Studying the use of nanohybrid to enhance PCM, but in different ratios, such as 70% nanowire, and 30% nanoparticles.

References

1. BP Statistical Review of World Energy, Full report – 2019. https://www.bp.com/content/dam/bp/business-sites/en/global/corporate/pdfs/energy-economics/statistical-review/bp-stats-review-2020-full-report.pdf
2. BP Statistical Review of World Energy, Full report – 2020. https://www.bp.com/content/dam/bp/business-sites/en/global/corporate/pdfs/energy-economics/statistical-review/bp-stats-review-2021-full-report.pdf
3. U.S. Energy Information Administration, Annual energy outlook 2022, (AEO2022 Narrative, 2022). https://www.eia.gov/outlooks/aeo/pdf/AEO2022_Narrative.pdf
4. International Energy Agency (IEA), World Energy Outlook 2021, Global Energy & CO2 Status Report 2021. https://iea.blob.core.windows.net/assets/4ed140c1-c3f3-4fd9-acae-789a4e14a23c/WorldEnergyOutlook2021.pdf
5. IRENA (2022), Renewable Energy Statistics 2022, The International Renewable Energy Agency, Abu Dhabi.
6. Gadhave, P., Pathan, F., Kore, S., & Prabhune, C. (2021). Comprehensive review of phase change material based latent heat thermal energy storage system. International Journal of Ambient Energy, 1–26. doi:10.1080/01430750.2021.1873848.
7. Tao, Y. B., & He, Y.-L. (2018). A review of phase change material and performance enhancement method for latent heat storage system. Renewable and Sustainable Energy Reviews, 93, 245–259. doi:10.1016/j.rser.2018.05.028.
8. Tofani, K. and Tiari, S., 2021. Nano-Enhanced Phase Change Materials in Latent Heat Thermal Energy Storage Systems: A Review. Energies, 14(13), p.3821.
9. Liu, W., Zhang, X., Ji, J., Wu, Y. and Liu, L., 2021. A Review on Thermal Properties Improvement of Phase Change Materials and Its Combination with Solar Thermal Energy Storage. Energy Technology, 9(7), p.2100169.
10. Sharma, N., Gaur, M. and Malvi, C., 2021. Application of phase change materials for cooling of solar photovoltaic panels: A review. Materials Today: Proceedings, 47, pp.6759-6765.
11. Yang, L., Huang, J. and Zhou, F., 2020. Thermophysical properties and applications of nano-enhanced PCMs: An update review. Energy Conversion and Management, 214, p.112876.
12. Preet, S., 2021. A review on the outlook of thermal management of photovoltaic panel using phase change material. Energy and Climate Change, 2, p.100033.

13. Hassan, A., Wahab, A., Qasim, M., Janjua, M., Ali, M., Ali, H., Jadoon, T., Ali, E., Raza, A. and Javaid, N., 2020. Thermal management and uniform temperature regulation of photovoltaic modules using hybrid phase change materials-nanofluids system. Renewable Energy, 145, pp.282-293.
14. Breeze, P., Chapter 8 - Solar Photovoltaic Technologies, in Solar Power Generation, P. Breeze, Editor. 2016, Academic Press. p. 51-55.
15. Siahkamari, L., Rahimi, M., Azimi, N. and Banibayat, M., 2019. Experimental investigation on using a novel phase change material (PCM) in micro structure photovoltaic cooling system. International Communications in Heat and Mass Transfer, 100, pp.60-66.
16. Sharma, G., Singh, M., Sehgal, S. and Sandhu, H., 2018. Experimental Study of Thermal Properties of PCM with Addition of Nano Particles, 0974-5645.
17. Nada, S., El-Nagar, D. and Hussein, H., 2018. Improving the thermal regulation and efficiency enhancement of PCM-Integrated PV modules using nano particles. Energy Conversion and Management, 166, pp.735-743.
18. Salem, M., Elsayed, M., Abd-Elaziz, A. and Elshazly, K., 2019. Performance enhancement of the photovoltaic cells using Al2O3/PCM mixture and/or water cooling-techniques. Renewable Energy, 138, pp.876-890.
19. Al-Waeli, A., Sopian, K., Chaichan, M., Kazem, H., Ibrahim, A., Mat, S. and Ruslan, M., 2017. Evaluation of the nanofluid and nano-PCM based photovoltaic thermal (PVT) system: An experimental study. Energy Conversion and Management, 151, pp.693-708.
20. Aurangzeb, M., Noor, F., Qamar, A., Shah, A., Kumam, P., Shah, Z. and Shutaywi, M., 2022. Investigation of enhancement in the thermal response of phase change materials through nano powders. Case Studies in Thermal Engineering, 29, p.101654.
21. Akhmetov, B., Navarro, M., Seitov, A., Kaltayev, A., Bakenov, Z. and Ding, Y., 2019. Numerical study of integrated latent heat thermal energy storage devices using nanoparticle-enhanced phase change materials. Solar Energy, 194, pp.724-741.
22. ZARMA, I., HASSAN, H., AHMED, M. and OOKAWARA, S., 2017. Investigation on Enhancement of Thermal Conductivity of Phase Change Material with Nanoparticles Addition for Thermal Energy Storage.
23. Sushobhan, B. and Kar, S., 2017. Thermal Modeling of Melting of Nano based Phase Change Material for Improvement of Thermal Energy Storage. Energy Procedia, 109, pp.385-392.

24. Liang, W., Wang, L., Zhu, H., Pan, Y., Zhu, Z., Sun, H., Ma, C. and Li, A., 2018. Enhanced thermal conductivity of phase change material nanocomposites based on MnO2 nanowires and nanotubes for energy storage. Solar Energy Materials and Solar Cells, 180, pp.158-167.
25. Karaipekli, A., Biçer, A., Sarı, A. and Tyagi, V., 2017. Thermal characteristics of expanded perlite/paraffin composite phase change material with enhanced thermal conductivity using carbon nanotubes. Energy Conversion and Management, 134, pp.373-381.
26. Chinnasamy, V. and Cho, H., 2022. Investigation on thermal properties enhancement of lauryl alcohol with multi-walled carbon nanotubes as phase change material for thermal energy storage. Case Studies in Thermal Engineering, 31, p.101826.
27. Bocharov, G., Gerasimov, D., Grigoriev, I., Dedov, A., Zverev, M. and Eletskii, A., 2020. Thermal Conductivity of Phase Changing Materials Doped with Carbon Nanotubes. Journal of Physics: Conference Series, 1683(3), p.032011.
28. Pasupathi, M., Alagar, K., P, M., M.M, M. and Aritra, G., 2020. Characterization of Hybrid-nano/Paraffin Organic Phase Change Material for Thermal Energy Storage Applications in Solar Thermal Systems. Energies, 13(19), p.5079.
29. Qu, Y., Wang, S., Zhou, D. and Tian, Y., 2020. Experimental study on thermal conductivity of paraffin-based shape-stabilized phase change material with hybrid carbon nano-additives. Renewable Energy, 146, pp.2637-2645.
30. BENLEKKAM, M. and NEHARI, D., 2022. Hybrid nano improved phase change material for latent thermal energy storage system: Numerical study. Archive of Mechanical Engineering, 69(1), pp.77–98.
31. Liu, X., Tie, J., Wang, Z., Xia, Y., Wang, C. and Tie, S., 2021. Improved thermal conductivity and stability of Na2SO4·10H2O PCMs system by incorporation of Al/C hybrid nanoparticles. Journal of Materials Research and Technology, 12, pp.982-988.
32. Aslfattahi, N., Saidur, R., Arifutzzaman, A., Abdelrazik, A., Samylingam, L., Sabri, M. and Sidik, N., 2020. Improved thermo-physical properties and energy efficiency of hybrid PCM/graphene-silver nanocomposite in a hybrid CPV/thermal solar system. Journal of Thermal Analysis and Calorimetry, 147(2), pp.1125-1142.
33. Arshad, A., Jabbal, M. and Yan, Y., 2020. Preparation and characteristics evaluation of mono and hybrid nano-enhanced phase change materials (NePCMs) for thermal management of microelectronics. Energy Conversion and Management, 205, p.112444.

34. Ibrahim, S., Ali, A., Hafidh, S., Chaichan, M., Kazem, H., Ali, J., Isahak, W. and Alamiery, A., 2022. Stability and thermal conductivity of different nano-composite material prepared for thermal energy storage applications. South African Journal of Chemical Engineering, 39, pp.72-89.
35. Zou, D., Ma, X., Liu, X., Zheng, P. and Hu, Y., 2018. Thermal performance enhancement of composite phase change materials (PCM) using graphene and carbon nanotubes as additives for the potential application in lithium-ion power battery. International Journal of Heat and Mass Transfer, 120, pp.33-41.
36. Sarbu, I., & Sebarchievici, C. (2018). A Comprehensive Review of Thermal Energy Storage. Sustainability, 10(1), 191.
37. Alva, G., Lin, Y., & Fang, G. (2018). An overview of thermal energy storage systems. Energy, 144, pp. 341–378.
38. Enescu, D., Chicco, G., Porumb, R., & Seritan, G. (2020). Thermal Energy Storage for Grid Applications: Current Status and Emerging Trends. Energies, 13(2), 340.
39. Ma, T., Li, Z., & Zhao, J. (2019). Photovoltaic panel integrated with phase change materials (PV-PCM): technology overview and materials selection. Renewable and Sustainable Energy Reviews, 116, pp. 109-406.
40. Irfan Lone, M., & Jilte, R. (2021). A review on phase change materials for different applications. Materials Today: Proceedings, 46, pp. 10980–10986.
41. Seto, D. B., Kristiawan, B., Ubaidillah, & Arifin, Z. (2021). Solar Cell Cooling with Phase Change Material (PCM) for Enhanced Efficiency: A Review. IOP Conference Series: Materials Science and Engineering, 1096(1), 012052.
42. Cheng, P., Chen, X., Gao, H., Zhang, X., Tang, Z., Li, A., & Wang, G. (2021). Different dimensional nanoadditives for thermal conductivity enhancement of phase change materials: Fundamentals and applications. Nano Energy, 85, 105948.
43. Qureshi, Z. A., Ali, H. M., & Khushnood, S. (2018). Recent advances on thermal conductivity enhancement of phase change materials for energy storage system: A review. International Journal of Heat and Mass Transfer, 127, pp. 838–856.
44. Kant, K., Shukla, A., Sharma, A., & Biwole, P. H. (2016a). Thermal response of poly-crystalline silicon photovoltaic panels: Numerical simulation and experimental study. Solar Energy, 134, pp.147–155.

45. Kant, K., Shukla, A., Sharma, A., & Biwole, P. H. (2016b). Heat transfer studies of photovoltaic panel coupled with phase change material. Solar Energy, 140, pp.151–161.
46. Popovici, C. G., Hudişteanu, S. V., Mateescu, T. D., & Cherecheş, N. C. (2016). Efficiency Improvement of Photovoltaic Panels by Using Air Cooled Heat Sinks. Energy Procedia, 85, pp. 425–432.
47. Sharaf, M., Yousef, M. S., & Huzayyin, A. S. (2022). Review of cooling techniques used to enhance the efficiency of photovoltaic power systems. Environmental Science and Pollution Research, 29(18), 26131–26159.
48. Juaidi, A., Manzano-Agugliaro, F., & Ibrik, I. H. (2016). An overview of renewable energy potential in Palestine. Renewable & Sustainable Energy Reviews, 65, 943–960.
49. Rabi, A., Ghanem, I. (2016). Solar Energy Production in Palestine // Pre Master Plan. Palestinian Environmental NGOs Network –Friends of Earth– Palestine (PENGON-FoE Palestine).
50. GLOBAL SOLAR ATLAS (2019), World Bank Group, Global Horizontal Irradiation, West Bank and Gaza, https://globalsolaratlas.info/download/west-bank-and-gaza.
51. Alsamamra. (2013). Statistical approach for modeling of daily global solar radiation on horizontal surfaces over Hebron City, Palestine. Journal of Technology Innovations in Renewable Energy.
52. NSRDB: National Solar Radiation Database, https://nsrdb.nrel.gov/data-viewer.
53. Zhou, J., Yi, Q., Wang, Y., & Ye, Z. (2015). Temperature distribution of photovoltaic module based on finite element simulation. Solar Energy, 111, 97–103.
54. Maan J B Buni, Ali A. K. Al-Walie, and Kadhem A. N. Al-Asadi. (2018). Effect of solar radiation on photovoltaic cell,‖ International Research Journal of Advanced Engineering and Science, Volume 3, Issue 3, pp. 47-51.
55. Nasrin, R., Hasanuzzaman, M., & Rahim, N. A. (2017). Effect of high irradiation on photovoltaic power and energy. International Journal of Energy Research, 42(3), 1115–1131.
56. Bahaidarah, H. M. S., Subhan, A., Gandhidasan, P., & Rehman, S. (2013). Performance evaluation of a PV (photovoltaic) module by back surface water cooling for hot climatic conditions. Energy, 59, 445–453.
57. Rahman, M. M., Hasanuzzaman, & Rahim, N. A. (2017). Effects of operational conditions on the energy efficiency of photovoltaic modules operating in Malaysia. Journal of Cleaner Production, 143, 912–924.

58. Charles Divyateja, B., Unnikrishnan, K. S., & Rohinikumar, B. (2021). Modelling and Numerical simulation of Nano-enhanced PV-PCM System for Heat Transfer Augmentation from the Panel. Journal of Physics: Conference Series, 2054(1), 012051.
59. Büyük Öğüt, E. (2009). Natural convection of water-based nanofluids in an inclined enclosure with a heat source. International Journal of Thermal Sciences, 48(11), 2063–2073.
60. Ansys Fluent Theory Guide. https://dl.cfdexperts.net/cfd_resources/Ansys_Documentation/Fluent/Ansys_Fluent_Theory_Guide.pdf.
61. Groulx, D., Biwole, P. H., & Bhouri, M. (2020). Phase change heat transfer in a rectangular enclosure as a function of inclination and fin placement. International Journal of Thermal Sciences, 151, 106260.
62. Vajjha, R. S., Das, D. K., & Namburu, P. K. (2010). Numerical study of fluid dynamic and heat transfer performance of Al2O3 and CuO nanofluids in the flat tubes of a radiator. International Journal of Heat and Fluid Flow, 31(4), 613–621.
63. Khanjari, Y., Pourfayaz, F., & Kasaeian, A. (2016). Numerical investigation on using of nanofluid in a water-cooled photovoltaic thermal system. Energy Conversion and Management, 122, 263–278.
64. Batchelor, G. K. (1977). The effect of Brownian motion on the bulk stress in a suspension of spherical particles. Journal of Fluid Mechanics, 83(1), 97–117.
65. Qiu, L., Zhu, N., Feng, Y., Michaelides, E. E., Żyła, G., Jing, D., Zhang, X., Norris, P. M., Markides, C. N., & Mahian, O. (2020). A review of recent advances in thermophysical properties at the nanoscale: From solid state to colloids. Physics Reports, 843, 1–81.
66. Zhu, D., Wang, L., Yu, W., & Xie, H. (2018). Intriguingly high thermal conductivity increment for CuO nanowires contained nanofluids with low viscosity. Scientific Reports, 8(1).
67. Hamilton, R., & Crosser, O. (1962). Thermal Conductivity of Heterogeneous Two-Component Systems. Industrial & Engineering Chemistry Fundamentals, 1(3), 187–191.
68. Fang, X., Ding, Q., Fan, L., Yu, Z., Xu, X., Cheng, G., Hu, Y., & Cen, K. (2014). Thermal Conductivity Enhancement of Ethylene Glycol-Based Suspensions in the Presence of Silver Nanoparticles of Various Shapes. Journal of Heat Transfer, 136(3).

69. Gu, B., Hou, B., Lu, Z., Wang, Z., & Chen, S. (2013). Thermal conductivity of nanofluids containing high aspect ratio fillers. International Journal of Heat and Mass Transfer, 64, 108–114.
70. Ghadikolaei, S., Yassari, M., Sadeghi, H., & Ganji, D. D. (2017). Investigation on thermophysical properties of Tio2–Cu/H2O hybrid nanofluid transport dependent on shape factor in MHD stagnation point flow. Powder Technology, 322, 428–438.
71. Faraji, H., Alami, M. E., & Arshad, A. (2021). Investigating the effect of single and hybrid nanoparticles on melting of phase change material in a rectangular enclosure with finite heat source. International Journal of Energy Research, 45(3), 4314–4330.
72. García-Fuente, M., González-Peña, D., & Alonso-Tristán, C.(2022). A Numerical Simulation of an Experimental Melting Process of a Phase-Change Material without Convective Flows. Applied Sciences, 12(7), 3640.
73. Reichl, C., Both, S., Mascherbauer, P., & Emhofer, J. (2022). Comparison of Two CFD Approaches Using Constant and Temperature Dependent Heat Capacities during the Phase Transition in PCMs with Experimental and Analytical Results. Processes, 10(2), 302.
74. Lee, Y., & Tay, A. a. O. (2012). Finite Element Thermal Analysis of a Solar Photovoltaic Module. Energy Procedia, 15, 413–420.
75. Wodołażski, A., Howaniec, N., Jura, B., Bak, A., & Smoliński, A. (2021). CFD Numerical Modelling of a PV–TEG Hybrid System Cooled by Air Heat Sink Coupled with a Single-Phase Inverter. Materials, 14(19), 5800.
76. Lamaamar, I., Tilioua, A., & Alaoui, A. E. H. (2022). Thermal performance analysis of a poly c-Si PV module under semi-arid conditions. Materials Science for Energy Technologies, 5, 243–251.

Appendixes:

Appendix A: ANSYS mesh details

Element Size: 3 mm. Multizone method then inflate this method. Mapped mesh type: Hexa.

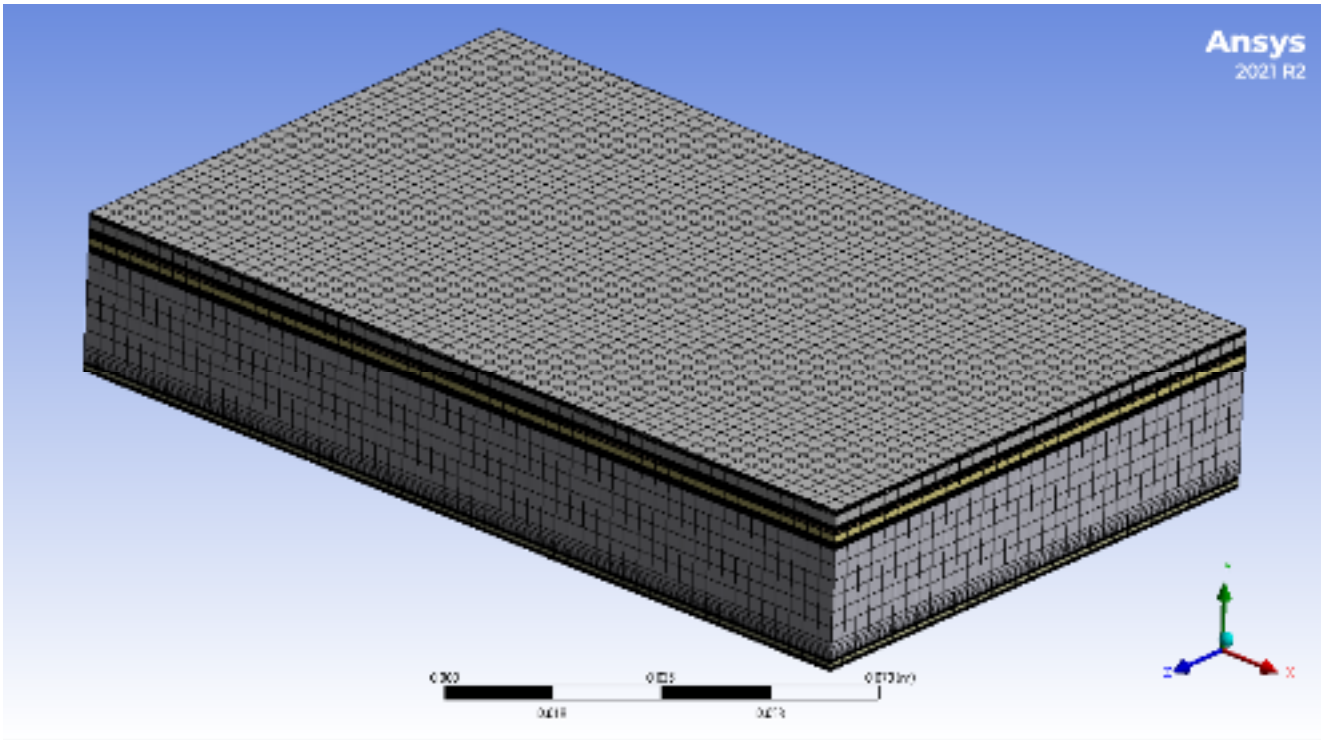

ANSYS meshing figure for PV-PCM

Appendix B: User-defined function (UDF)

UDF for thermophysical properties of PCM:

```
#include "udf.h"


DEFINE_SPECIFIC_HEAT(my_user_cp, T, Tref, h, yi)
{
real cp;
real B, H, D;
if (T < 297.75)
{
cp = 1800.00;
}
else if (T < 301.75)
{
B = (T-297.75)/4;
H = pow((T-299.75),2);
D = exp((-H/4)/3.544907702);
cp = 1800.00+(600.00*B)+(232000.00*D);
}
else
{
cp = 2400.00;
}
*h = cp*(T-Tref);
return cp;
```

```
}
```

```
#include "udf.h"

DEFINE_PROPERTY(cell_density,c,t)

{

real B, rho;

real temp = C_T(c,t);

if (temp < 297.75)

{

rho = 785.00;

}

else if (temp < 301.75)

{

B = (temp-297.75)/4;

rho = 785.00-(36.00*B);

}

else

{

rho = 749.00;

}

return rho;

}
```

```
#include "udf.h"

DEFINE_PROPERTY(cell_viscosity,c,t)

{

real mu_lam, A, B;

real temp = C_T(c,t);

if (temp < 297.75)
```

```
{
mu_lam = 179800.0018;
}
else if (temp < 301.75)
{
B = (temp-297.75)/4;
A = (100000*(pow((1-B),2)))/((pow(B,3))+0.001);
mu_lam = 0.001798*(1+A);
}
else
{
mu_lam = 0.001798;
}
return mu_lam;
}
```

```
#include "udf.h"
DEFINE_PROPERTY(cell_thermal_conductivity,c,t)
{
real ktc;
real temp = C_T(c,t);
if (temp < 297.75)
{
ktc = 0.19;
}
else if (temp < 301.75)
{
ktc = 0.19-(0.01*((temp-297.75)/4));
```

```
}
else
{
ktc = 0.18;
}
return ktc;
}
```

UDF for thermophysical properties of NPCM ($\varphi = 0.5\%$):

```
#include "udf.h"
#define FI 0.005

DEFINE_SPECIFIC_HEAT(my_user_cpNANO1, T, Tref, h, yi)
{
real cp;
real B, rho_pcm, rho_nano, D, H, cp_pcm;
if (T < 297.75)
{
rho_nano = (10500*FI)+(785*(1-FI));
cp = ((2467500*FI)+(785*(1-FI)*1800))/(rho_nano);
}
else if (T < 301.75)
{
B = (T-297.75)/4;
rho_pcm = 785.00-(36.00*B);
rho_nano = (FI*10500)+((1-FI)*rho_pcm);
H = pow((T-299.75),2);
D = exp((-H/4)/3.544907702);
cp_pcm = 1800.00+(600.00*B)+(232000*D);
```

```
cp = ((2467500*FI)+((1-FI)*rho_pcm*cp_pcm))/rho_nano;
}
else
{
rho_nano = (10500*FI)+(749*(1-FI));
cp = ((2467500*FI)+(749*(1-FI)*2400))/(rho_nano);
}
*h = cp*(T-Tref);
return cp;
}
```

```
#include "udf.h"
#define FI 0.005

DEFINE_PROPERTY(cell_densityNANO1,c,t)
{
real rho;
real rho_pcm, B;
real temp = C_T(c,t);
if (temp < 297.75)
{
rho = (FI*10500)+((1-FI)*785);
}
else if (temp < 301.75)
{
B = (temp-297.75)/4;
rho_pcm = 785.00-(36.00*B);
rho = (FI*10500)+((1-FI)*rho_pcm);
}
else
```

```
{
rho = (FI*10500)+((1-FI)*749);
}
return rho;
}
```

```
#include "udf.h"
#define FI 0.005
DEFINE_PROPERTY(cell_viscosityNANO1,c,t)
{
real mu_lam;
real mu_lamPCM, A, B;
real temp = C_T(c,t);
if (temp < 297.75)
{
mu_lamPCM = 179800.0018;
mu_lam = (1+(2.5*FI)+(6.2*(pow(FI,2))))*mu_lamPCM;
}
else if (temp < 301.75)
{
B = (temp-297.75)/4;
A = (100000*(pow((1-B),2)))/((pow(B,3))+0.001);
mu_lamPCM = 0.001798*(1+A);
mu_lam = (1+(2.5*FI)+(6.2*(pow(FI,2))))*mu_lamPCM;
}
else
{
mu_lamPCM = 0.001798;
mu_lam = (1+(2.5*FI)+(6.2*(pow(FI,2))))*mu_lamPCM;
}
```

```
return mu_lam;
}
```

```
#include "udf.h"
#define FI 0.005

DEFINE_PROPERTY(cell_thermal_conductivityNANO1,c,t)
{
real ktc;
real ktc_pcm, B;
real temp = C_T(c,t);
if (temp < 297.75)
{
ktc_pcm = 0.19;
ktc = ktc_pcm*((429+(2*ktc_pcm)-(2*FI*(ktc_pcm-429)))/(429+(2*ktc_pcm)+(FI*(ktc_pcm-429))));
}
else if (temp < 301.75)
{
B = (temp-297.75)/4;
ktc_pcm = 0.19-(0.01*B);
ktc = ktc_pcm*((429+(2*ktc_pcm)-(2*FI*(ktc_pcm-429)))/(429+(2*ktc_pcm)+(FI*(ktc_pcm-429))));
}
else
{
ktc_pcm = 0.18;
ktc = ktc_pcm*((429+(2*ktc_pcm)-(2*FI*(ktc_pcm-429)))/(429+(2*ktc_pcm)+(FI*(ktc_pcm-429))));
}
return ktc;
}
```

```
#include "udf.h"

#define FI 0.005


DEFINE_PROPERTY(cell_thermal_conductivityNANO11,c,t)

{

real ktc;

real ktc_pcm, B;

real temp = C_T(c,t);

if (temp < 297.75)

{

ktc_pcm = 0.19;

ktc = ktc_pcm*((429+(16.12027918*ktc_pcm)-(16.12027918*FI*(ktc_pcm-
429)))/(429+(16.12027918*ktc_pcm)+(FI*(ktc_pcm-429))));

}

else if (temp < 301.75)

{

B = (temp-297.75)/4;

ktc_pcm = 0.19-(0.01*B);

ktc = ktc_pcm*((429+(16.12027918*ktc_pcm)-(16.12027918*FI*(ktc_pcm-
429)))/(429+(16.12027918*ktc_pcm)+(FI*(ktc_pcm-429))));

}

else

{

ktc_pcm = 0.18;

ktc = ktc_pcm*((429+(16.12027918*ktc_pcm)-(16.12027918*FI*(ktc_pcm-
429)))/(429+(16.12027918*ktc_pcm)+(FI*(ktc_pcm-429))));

}

return ktc;

}
```

UDF for thermophysical properties of HNPCM ($\varphi = 0.5\%$):

```
#include "udf.h"
#define FI 0.0025
#define FII 0.0025

DEFINE_SPECIFIC_HEAT(my_user_cpNANO1, T, Tref, h, yi)
{
real cp;
real B, rho_pcm, rho_nano, D, H, cp_pcm;
if (T < 297.75)
{
rho_pcm = 785;
cp_pcm = 1800;
rho_nano = ((1-FII)*(((1-FI)*rho_pcm)+(10500*FI)))+(10500*FII);
cp = (((1-FII)*(((1-FI)*rho_pcm*cp_pcm)+(FI*10500*235)))+(FII*10500*235))/rho_nano;
}
else if (T < 301.75)
{
B = (T-297.75)/4;
rho_pcm = 785.00-(36.00*B);
rho_nano = ((1-FII)*(((1-FI)*rho_pcm)+(10500*FI)))+(10500*FII);
H = pow((T-299.75),2);
D = exp((-H/4)/3.544907702);
cp_pcm = 1800.00+(600.00*B)+(232000*D);
cp = (((1-FII)*(((1-FI)*rho_pcm*cp_pcm)+(FI*10500*235)))+(FII*10500*235))/rho_nano;
}
else
{
rho_pcm = 749;
```

```
cp_pcm = 2400;
rho_nano = ((1-FII)*(((1-FI)*rho_pcm)+(10500*FI)))+(10500*FII);
cp = (((1-FII)*(((1-FI)*rho_pcm*cp_pcm)+(FI*10500*235)))+(FII*10500*235))/rho_nano;
}
*h = cp*(T-Tref);
return cp;
}
```

```
#include "udf.h"
#define FI 0.0025
#define FII 0.0025

DEFINE_PROPERTY(cell_densityNANO1,c,t)
{
real rho;
real rho_pcm, B;
real temp = C_T(c,t);
if (temp < 297.75)
{
rho_pcm = 785;
rho = ((1-FII)*(((1-FI)*rho_pcm)+(10500*FI)))+(10500*FII);
}
else if (temp < 301.75)
{
B = (temp-297.75)/4;
rho_pcm = 785.00-(36.00*B);
rho = ((1-FII)*(((1-FI)*rho_pcm)+(10500*FI)))+(10500*FII);
}
else
```

```
{
rho_pcm = 749;
rho = ((1-FII)*(((1-FI)*rho_pcm)+(10500*FI)))+(10500*FII);
}
return rho;
}
```

```
#include "udf.h"
#define FI 0.0025
#define FII 0.0025

DEFINE_PROPERTY(cell_viscosityNANO1,c,t)
{
real mu_lam;
real mu_lamPCM, A, B, Y, Z;
real temp = C_T(c,t);
if (temp < 297.75)
{
mu_lamPCM = 179800.0018;
Y = pow((1-FI),2.5);
Z = pow((1-FII),2.5);
mu_lam = mu_lamPCM/(Y*Z);
}
else if (temp < 301.75)
{
B = (temp-297.75)/4;
A = (100000*(pow((1-B),2)))/((pow(B,3))+0.001);
mu_lamPCM = 0.001798*(1+A);
Y = pow((1-FI),2.5);
```

```
Z = pow((1-FII),2.5);
mu_lam = mu_lamPCM/(Y*Z);
}
else
{
mu_lamPCM = 0.001798;
Y = pow((1-FI),2.5);
Z = pow((1-FII),2.5);
mu_lam = mu_lamPCM/(Y*Z);
}
return mu_lam;
}
```

```
#include "udf.h"
#define FI 0.0025
#define FII 0.0025

DEFINE_PROPERTY(cell_thermal_conductivityNANO1,c,t)
{
real ktc;
real ktc_pcm, B, ktc_b;
real temp = C_T(c,t);
if (temp < 297.75)
{
ktc_pcm = 0.19;
ktc_b = ktc_pcm*((429+(2*ktc_pcm)-(2*FI*(ktc_pcm-429)))/(429+(2*ktc_pcm)+(FI*(ktc_pcm-429))));
ktc = ktc_b*((429+(16.12027918*ktc_b)-(16.12027918*FII*(ktc_b-
429)))/(429+(16.12027918*ktc_b)+(FII*(ktc_b-429))));
}
else if (temp < 301.75)
```

```
{

B = (temp-297.75)/4;

ktc_pcm = 0.19-(0.01*B);

ktc_b = ktc_pcm*((429+(2*ktc_pcm)-(2*FI*(ktc_pcm-429)))/(429+(2*ktc_pcm)+(FI*(ktc_pcm-429))));

ktc = ktc_b*((429+(16.12027918*ktc_b)-(16.12027918*FII*(ktc_b-
429)))/(429+(16.12027918*ktc_b)+(FII*(ktc_b-429))));

}

else

{

ktc_pcm = 0.18;

ktc_b = ktc_pcm*((429+(2*ktc_pcm)-(2*FI*(ktc_pcm-429)))/(429+(2*ktc_pcm)+(FI*(ktc_pcm-429))));

ktc = ktc_b*((429+(16.12027918*ktc_b)-(16.12027918*FII*(ktc_b-
429)))/(429+(16.12027918*ktc_b)+(FII*(ktc_b-429))));

}

return ktc;

}
```
